The Waiting Game: Elk avoid predator encounters at fine spatial scales

by

Mitchell James Flowers

A thesis submitted in partial fulfillment of the requirements for the degree of

Master of Science

in

Ecology

Department of Biological Sciences

University of Alberta

Abstract

Ungulates are known to avoid predation by grouping up, increasing vigilance, and reducing residency time among preferred habitats. Similarly, shifting return rates may represent a means of pre-emptively minimizing exposure to risk by being less predictable on the landscape to predators. We hypothesized that across seasons elk (*Cervus canadensis*) would be attracted to areas with high forage resulting in shorter revisit times, whereas revisit times would be longer to sites where perceived (indirect) predation risk was high, or where predators were observed on the cameras (direct risk) between elk events. With data from remote cameras (n = 44) distributed across the Ya Ha Tinda ranch in Alberta, Canada (2017–2018), we used Cox proportional hazards models to examine what influenced herd-level variation in elk revisit times during both winter and summer. After controlling for seasonal shifts in movements and/or distribution with data from GPS-collared resident elk, we assessed whether elk stayed away from sites recently visited by predators and how interactions between site characteristics (*e.g.* landcover types, edge density, distance to human infrastructure) and elk group size might further influence revisit times. Best supported winter models revealed sites were revisited by elk 61% sooner when surrounded by a high proportion of grasslands and revisited 68% longer when wolves (*Canis lupus*) occurred between elk, but this delay was consistently less among sites predominantly surrounded by grassland. During summer, elk revisit times among sites surrounded by higher edge densities were 12% longer, where as revisit times of elk to a site where a predator had previously occurred increased by 57% when the predator was a wolf, 40% when it was a bear (*Ursus arctos*), and 66% when it was a cougar (*Puma concolor*). Measuring fine-scale temporal dynamics in elk use across a risky landscape may help us better understanding how they avoid predator encounters altogether when coping with frequent changes in predation risk.

Preface

This thesis is an original work by Mitchell J. Flowers. Field data were collected during this MSc project (M. Flowers and E. Merrill, 2016-2019). Field methods were in accordance with the Canadian Council on Animal Care Guidelines and approved by the University of Alberta BioScience Animal Care and Use Committee (Protocol # AUP AUP00000624).

To date, no manuscripts have been submitted for publication.

Acknowledgements

This project would not have been possible without the funding and in-kind support from Alberta Conservation Association − Grants in Biodiversity, Natural Science and Engineering Research Council, Safari Club International − Northern Alberta Chapter, Alberta Environment and Parks, and Parks Canada.

I am incredibly grateful to Dr. Evelyn Merrill for giving me this opportunity. I would not have come close to finishing this program without her guidance, diligence, expertise, and understanding. Thank you for challenging me and for having more patience than I often deserved. Thank you to Andy Derocher for serving on my committee, providing valuable feedback, and posing important questions along the way. Additional thanks to Stan Boutin for acting as my external examiner.

Thank you to Rick and Jean Smith, for welcoming yet another round of grad students into their lives and not minding the arsenal of trail cameras that glimpsed into the private lives of their wild neighbours (and occasionally, their dogs). Even though I never stayed for very long, it always felt like coming home. The ranch will not be the same without you. I'd also like to thank a few others at Parks Canada, in particular Blair Fyten and Jesse Whittington, for their hospitality and their in-kind and logistical support during the early days of this project.

Thank you to all of my research technicians, Eilidh Smith, Jessica Melsted, Prashanna Pokharel, and Kayla Kuefler. As exciting as some sequences can be, it was not easy, and I could not have classified all those images without you. I'd also like to thank those who have been, and still are, members of the Merrill, Boyce, Boutin, and Hebblewhite labs. Thank you for all your help in the field, all your advice in the office, and all your friendship elsewhere. In particular (but

no particular order), I would like to thank April Martinig, Kara MacAulay, Phil Walker, Maria Dobbin, Sean Konkolics, Darcy Doran−Myers, Conor Mallory, Meghan Beale, Michael Peers, Yasmine Majchrzak, Mateen Hessami, Hans Martin, Camille Roberge, and Eric Spilker. Special thanks to Jacky Normandeau for being on-call to help format this thesis during the final days before its submission. You are too generous, and I can't thank you enough. And another special thanks to Samantha Widmeyer, for so many things.

Finally, I have to thank my family. Thank you, Mom, Dad, and Stef, for all the best parts of me that are so difficult to describe and so easily taken for granted, and for all the time we spent on Wren Lake. That was my wilderness. I doubt I'd be writing this if it hadn't been.

And how could I forget, Ghide (*Rhacodactylus leachianus*). Thank you for bringing a small piece of the wild into my home and always reminding me to slow down. I look forward to spending the next few decades together.

Table of Contents

The Waiting Game: Elk avoid predator encounters at fine spatial scales

Introduction.....1

Methods.....4

Study Area.....4

Camera distribution, specifications, and image classification.....6

Modelling elk revisit times.....8

Seasonal elk movements and distribution.....10

Elk group characteristics and predator occurrence.....12

Camera site characteristics.....12

Results.....13

Image classification summary.....13

Seasonal elk movements and distribution.....14

Modelling elk revisit times.....15

Discussion.....17

Bibliography.....35

Supplementary Material.....45

List of Tables

Table 1. Hypotheses and predictions of the effects of movements, site preferences, predation risk, and reproductive status on revisit times of non-migratory elk to camera sites in the Ya Ha Tinda range along the east slope of the Rocky Mountains, Alberta..... 23

Table 2. Covariates used for modelling elk revisit times with photographs of elk and their predators collected at remote cameras across the winter range of the Ya Ha Tinda, along the eastern slopes of the Rocky Mountains of Alberta, Canada. If data sources are not indicated (--), covariates were created by the authors with project data..... 24

Table 3. Summary of model selection results based on AIC for predicting daily movement rates of GPS-collared elk (metres/2 hr) in winter and summer of 2017. Top models shown in bold..... 25

Table 4. Model selection results based on AIC for predicting revisit times with a single metric related to elk movements or space use in winter and summer. All models include a random effect for location ID..... 26

Table 5. Model selection results based on AIC for predicting revisit times of elk at remote camera sites across the Ya Ha Tinda during winter (1-December to 30-April). All models include a random effect for location ID. The top models are shown in bold. See variable definitions in Table 2 and all other candidate models tested in Appendix 11..... 26

Table 6. Beta coefficients (± SE) and hazard ratios (HR ± CI [95%]) of the best models predicting revisit times of elk at remote cameras during winter and summer across the Ya Ha Tinda ranch property (2017–2018). Both models include location ID as a random effect. Hazard ratios with values >1 indicate a *decrease* in revisit times (of 1–HR) and those with values <1 indicate an *increase* in revisit times. For example, the presence of wolves increases revisit times by 68% during winter (1 – 0.32 = 0.68)..... 27

Table 7. Summary of model selection results based on AIC for predicting revisit times of elk at remote camera sites across the Ya Ha Tinda during summer (1-June to 15-Sept). All models include a random effect for location ID. Top model is shown in bold. See all other candidate models tested in Appendix 12..... 27

List of Figures

Figure 1. The winter range of Ya Ha Tinda, with an impressive view into Banff National Park. Photographed by Jacalyn Normandeau..... 28

Figure 2. Distribution of remote cameras (n = 44) across the winter range of the Ya Ha Tinda's partially migratory elk herd, along the eastern slopes of the Rocky Mountains, Alberta, Canada. Cameras were distributed within the minimum convex polygon of pooled 2-hr relocations of GPS-collared elk (n = 20/year) from the winters of 2010 to 2015..... 29

Figure 3. Mean daily movement rates (m/2 hr) of GPS-collared elk (n = 20) fitted with linear, quadratic, and cubic functions from (A) 1 December to 30 April 2017 and (B) 1 June to 17 September 2017. Winter data was best fit by the null model (*i.e.*, seasonal average), indicating no seasonal trend (ΔAIC > 2; Table 3). As a result, daily movement rates were not included as a covariate when modelling revisit times in winter. Summer data was best fit by the quadratic model (ΔAIC > 14; Table 3). Values predicted by the quadratic model were then used for determining the average daily movement rate between elk observations used to model revisit times in summer. Top models for each season are shown with solid lines..... 30

Figure 4. (A) Proportion of 2-hr relocations of GPS-collared elk (n =21) within the camera area and (B) summer home range sizes (km^2) of GPS-collared elk (n =21) across the very early (*i.e.*, calf-rearing; 1 June – 25 June;), early (26 June – 25 July), middle (26 July – Aug 24), and late summer (25 Aug – 15 Sept) periods. To view the geographical distributions of GPS relocations and home ranges across summer periods, refer to Appendix 14..... 31

Figure 5. Hazard (or likelihood) of any elk revisiting a camera site in winter with respect to the proportion of nearby grasslands, interacted with wolves being present (1) or absent (0). Shaded regions represent 95% confidence limits..... 32

Figure 6. Cumulative hazard curves and 95% confidence limits for any elk revisiting a camera site in (A) winter when a wolf was observed (blue) or not observed (orange) between elk events or in summer when a wolf (B), cougar (C) and (D) bear was observed (blue) or not observed (orange) between elk events..... 33

Figure 7. Hazard (or likelihood) of any elk revisiting a camera site in summer with respect to (A) increasing edge densities and (B) larger group sizes with 95% confidence limits (shaded regions). The baseline hazard ($y = 1$) is shown as a dashed horizontal line..... 34

THE WAITING GAME: ELK AVOID PREDATOR ENCOUNTERS AT FINE SPATIAL SCALES

INTRODUCTION

Large herbivores respond to changes in the availability of their resources over time and space. Resource utilization functions provide a means of mapping animal distributions based on the environment using either direct observations of use or estimating use based on animal selection (Marzluff et al. 2004, Signer et al. 2017, Hooten et al. 2013, Millspaugh et al. 2006). However, resource utilization distributions provide little mechanistic understanding of how these patterns arise from animal behavior to help inform conservation efforts (Greggor et al. 2016). Recent improvement of sequential sampling of animals based on high-resolution spatiotemporal data through GPS technology has led to an increasing emphasis on how animal space use emerges from characteristics of animal movements (Tomkiewicz et al. 2010, Kays et al. 2015). In particular, a clearer understanding of what influences not only where animals choose to go (*i.e.*, selection) but also how long they stay and how often they return is key to understanding strategies for space use in heterogeneous environments (Benhamou and Riotte-Lambert 2012, Bracis et al. 2018).

Two common metrics used in describing the fine-scale movements of individual animals in space are residence time and return time (Van Moorter et al. 2016, English et al. 2014, Kapota et al. 2017, Bar-David et al. 2009). Residence time is the time spent within a confined patch or area (Sur et al., 2014, Seidel and Boyce 2015, Hoover et al. 2019). High residence time can result from either slow or highly tortuous movements in an area indicating a more area-restricted search (Barraquand and Benhamou 2008). Optimal foraging theory predicts that a herbivore should remain in an area as long as the marginal rate of forage intake resulting from depletion is greater than the average value of the landscape (Charnov 1976). However, efficient use of resources may be traded-off against relative risks of predation (Brown and Kotler 2004, Kie 1999). Return time

or recursion rates are defined as the time it takes an individual to revisit a previously visited site (Berger-Tal and Bar-David 2015). The rate or time to return is assumed to indicate the level of attraction to a site. For example, elk (*Cervus canadensis*) returned most frequently to high productivity patches and exhibited directed movements toward these patches (Seidel and Boyce 2015). Return times by herbivores also may reflect timing of re-growing patterns of vegetation, which is key to maintaining consumption of high-quality forage (Benhamou and Riotte-Lambert 2012, Martin et al. 2015). Short residency rates and high return rates may make prey species less predictable on the landscape to predators (Bowyer et al. 1999, Anderson et al. 2008). Consequently, similar patterns of overall resource use may emerge from different behavioral tactics of herbivores that have implications for forage-predator trade-offs.

To date, most studies decomposing movement characteristics of resource use into residence time and return time have been based on movement paths of individual animals with GPS telemetry because of the sequential sampling this approach offers (Anderson et al. 2008, English et al. 2014, Martin et al. 2015, Bracis et al. 2018, Hoover et al. 2019, Wolf et al. 2009). However, residence and return times are sensitive to sampling frequency of animal locations (Seidel and Boyce 2015), and identifying patches perceived by herbivores is not straight forward (Barraquand et al. 2008). We illustrate a second approach to quantify return times at the level of the population, or revisit times, involving detections of elk at remote camera sites. Remote cameras have been used to assess occupancy, intensity of use, activity patterns and to estimate animal density (Carhone et al. 2002, Jennelle et al. 2002, Chandler et al. 2013, Cusack et al. 2015, Frey et al. 2017, Burton et al. 2015, Moeller et al. 2018), but to our knowledge they have not been used to assess revisit times, which we hypothesized reflect attraction to a site. However, unlike sampling return times of marked individuals (Anderson et al. 2008, English et al. 2014, Martin et al. 2015, Van Moorter et al. 2016),

revisit times to fixed sites measured for a population is a function not only of the attraction to a site, but of the number of animals whose movements overlap a camera site (*i.e.,* animal density) and the movement rates of animals (Jennelle et al. 2002, Parsons et al. 2017, Bischof et al. 2014, Moeller et al. 2018).

In this study, we used measures of elk revisit times derived from remote camera sites and concomitant metrics of distribution and movement rates of GPS-collared elk to assess changes in the influence of site characteristics and predator occurrence on revisit times of resident elk at the Ya Ha Tinda ranch in Alberta, Canada, along the eastern foothills of the Rocky Mountains, while independently controlling for the seasonal shifts in elk distribution in the camera grid and movement rates (Moeller et al. 2018). The Ya Ha Tinda is one the few remaining native fescue (*Festuca campestris*) grasslands in Alberta, Canada and is inhabited by a partially migratory elk herd. The Ya Ha Tinda elk herd has declined over the past two decades to about 400 elk during this study with about 50% of the elk migrating in summer either westward to high elevations in Banff National Park or eastward to lower elevation industrial forest lands (Hebblewhite et al. 2006, Eggeman et al. 2016, Berg 2019).

To assess what influenced how often sites were revisited by elk, we first examined within-season movement and distributions characteristics that were derived from GPS-collared elk inhabiting the Ya Ha Tinda, and when we found these to influence time to revisit, these metrics were considered part of the null model against which all ecological models were compared. We then addressed 7 ecological hypotheses affecting revisit times related to site characteristics, group size and composition, and direct and indirect predation risk and their interactions (Table 1). We hypothesized that across seasons elk would be attracted to areas with high forage resulting in shorter revisit times, whereas revisit times would be longer to sites where perceived (indirect)

predation risk was high, or where predator presence were observed on the cameras (direct risk). We used edge density as a metric of indirect predation risk because cougars (*Puma concolor*) and wolves (*Canis lupus*) are known to hunt or bed along forest edges (Kortello et al. 2007, Laundré and Hernandez 2003, Holmes and Laundré 2006) and elk at the Ya Ha Tinda have shown higher vigilance near timber (Robinson and Merrill 2013). Resident elk also use areas close to human infrastructure as a human refuge because predators, particularly wolves, avoid human activity (Hebblewhite and Merrill 2008, Robinson et al. 2010). Alternatively, elk may avoid human activity and roads (Frair et al. 2008, Wisdom et al. 2018, Prokopenko et al. 2017) so we assessed whether revisit times were longer at camera sites near human infrastructure. Finally, we hypothesized that group size would moderate (*i.e.*, interaction) direct and indirect predator effects.

METHODS

Study area

The Ya Ha Tinda is a 40-km^2 rough fescue (*Festuca campestris*) grassland situated along the eastern slopes of the Rocky Mountains, northeast of Banff National Park in Alberta, Canada (Fig. 1). Within the area the Ya Ha Tinda Ranch is a Parks Canada working horse ranch and the winter range of the partially migratory Ya Ha Tinda elk herd (Hebblewhite et al. 2006). The ranch itself is federally managed but wildlife management in the area falls within provincial jurisdiction. A gravel road providing access to the ranch facilities along the Red Deer River was recently (2017) re-routed through the middle of grasslands but motorized vehicle use is otherwise restricted. The provincial Bighorn campground on the eastern edge of the Ya Ha Tinda has equestrian use throughout the summer.

The central fescue grasslands on the north side of the Red Deer River have gentle rolling topography at 1,500-m surrounded immediately by foothills up to 2,400-m. The winter range

includes grasslands (13%) with peripheral stands of willow (*Salix* spp.) and bog birch (*Betula glandulosa*) shrublands (14%), aspen stands (3%), and conifer stands (37%) of lodgepole pine (*Pinus contorta*) at low elevations and Englemann spruce (*Picea engelmannii*) in the adjacent high elevations (Hebblewhite et al. 2006). Chinook winds occur frequently in winter, which reduces snowpack below 25-cm and often leaves the grasslands without snow (Morgantini 1995). During the study, mean daily temperatures across both winters (Dec to Mar) were –7°C (ranging from –27°C to 10°C), which was consistent with the 10-year average (2008 to 2018) of –6°C that ranged from 34°C to 11°C (Scalp Creek Station, Government of Alberta 2019). Snow depths during the study period ranged from 0 to 47-cm, with an average of 17-cm across winters (Sundre A Station, Government of Alberta 2019). Mean daily temperature across both summers (June to Sept) was 9.1°C, which was also similar to the 10-year average of 9.3°C (both periods ranging from –6°C to 22°C). Summer precipitation averaged 2.34 mm/day.

Elk abundance on the Ya Ha Tinda winter range have declined from ~1,400 since the early 2000s to current estimates of 411 ± 54 from 2014 – 2016 (Berg 2019). White-tailed deer (*Odocoileus virginianas*), mule deer (*O. hemoinus*) and bighorn sheep (*Ovis canadensis*) are also abundant in the area. Domestic horses are also present year-round in the fenced pastures within the ranch property. Hunting of elk and other ungulates is prohibited in the fenced pastures of the Ya Ha Tinda and anywhere within 350-m of the ranch road (*i.e.,* the Ya Ha Tinda wildlife sanctuary). Elk hunting is not permitted on the Ya Ha Tinda except by Indigenous people. Antlered and antlerless special licenses are permitted for elk in the surrounding Wildlife Management Units but did not coincide with the summer and winters periods used for this study (Government of Alberta 2017).

Major predators of elk in the area include wolves, grizzly (*Ursus arctos*) and black bears (*U. americanus*) and cougars. Wolf populations returned to Banff National Park in the mid 1980s and have remained relatively stable in recent years, despite substantial hunter harvest and trapping throughout surrounding public lands (Bassing et al. 2019). Grizzly bears currently are a threatened species in Alberta, with recent density estimates ranging from 4.79 to 5.25 bears per 1000-km^2 across the province (Alberta Environment and Parks 2016). Cougars have been expanding their range across Alberta for the past two decades (Knopff et al. 2014) and densities vary from 15 to 30 individuals/1000-km^2 from the west to the east of Ya Ha Tinda, respectively (Alberta Environment and Sustainable Resource Development 2012).

Camera distribution, specifications, and image classification

We used 44 Reconyx HC500 (Holmen, WI, USA) motion-activated cameras within the minimum convex polygon (65 km^2) of pooled 2-hr relocations of GPS-collared elk (n = 20/year) from the winters of 2010 to 2015 (hereafter, camera area). Seven cameras previously established within the study on horse trails were incorporated into the study. The remaining 37 cameras (31 in 2017, with an additional 6 in 2018) were distributed within a 2.5-km^2 grid system across the study area among cells classified by two strata: vegetation type (open canopy, closed canopy, and edge) and distance from human infrastructure (Fig. 2; Appendix 1). Open-canopy cells were dominated (≥ 50%) by grassland, shrub, or burned areas (<15 years since burning) and closed-canopy areas were dominated by coniferous and deciduous forests. Edge included areas ≤ 20-m from either side of the interface between open and closed patches >250-m^2, which corresponded to edge widths of 40-m that characterize cougar selection of transition zones (Holmes and Laundré 2006). Distance to human activity was measured as the straight-line distance from the centroid of the cell to the nearest point of the perimeter fencing surrounding the ranch buildings and classified as 0–1-km,

>1–3-km, and >3–7-km. Given these criteria are not mutually exclusive, a single cell could represent more than one vegetation type and contain up to 3 cameras (*i.e.,* 1 for each vegetation type). Specific sites for camera installation within each cell were chosen in the field within a 100-m buffer of an initially random location, with 11 cameras (25%) on lightly used game trails and 26 (57%) on the nearest available tree. Cameras were positioned so the field of view represented the edge, grassland or forest cell classification.

Cameras recorded data in winter (1 December – 30 April) and summer (1 June – 15 September) in 2017 and 2018 and followed protocols described by Steenweg et al. (2016). Cameras operated 24 hours per day at the highest sensor sensitivity and were set to take 5 pictures in rapid succession when triggered with no delay between consecutive triggers. Cameras were deployed to maximize the zone of detection and minimize the probability of not capturing faster moving animals by angling cameras at 45° and placing them approximately 2.5-m from the presumed line of travel at each site. This arrangement on trails has been shown to be effective at capturing the passage of large mammals moving at high speeds (Ladle et al. 2017). To prevent false triggers from windblown vegetation, all grasses and shrubs were cleared to a height of 5−10-cm at a distance of at least 5 m and angle of approximately 60° to encompass the full field of view (40°) for each device.

Images were analyzed using Timelapse software (Greenberg and Goudin 2015). Image sequences separated by at least 10 mins were considered independent events for all species regardless of whether the same individuals were being photographed. We applied a 10-min threshold between events because a high number of events can result from intense use by a single individual or moderate use by several (Steenweg et al. 2016). Images of elk were classified by event ID, number, sex, and age of individuals. Elk events separated by >10 minutes were not

considered a new event if the same individuals (as recognized by unique collar IDs or antler configurations) were present between consecutive sequences in the same position. This could occur when individual elk closer to the camera were photographed intermittently while the rest of the herd remained bedded down in the background. When classifying groups of animals, the entire sequence of images was considered because an entire group may not be present in any single photograph of a given sequence.

Modelling elk revisit times

We used Cox proportional hazard models to relate revisit times of any elk to a camera site to elk movements and space use, elk group size and composition, site variables, and whether predators had visited the site. We developed seasonal models separately because we expected habitat selection and elk densities to differ between seasons and limited the extent of the seasons to avoid the elk migration period (Hebblewhite et al. 2016). An "event" was defined as an image of an elk or group of elk detected by the camera. Time of the event was obtained from time stamps generated with each photograph. The time to an event (hereafter revisit time) was determined as the time between two consecutive elk events >12 hrs apart at a camera site. Given elk are crepuscular, using a minimum threshold of 12 hours for revisit times assumed elk had time to leave the site such that shorter revisit times did not represent multiple detections of elk that had yet to leave a site (*i.e.* an artifact of long residency times; Van Moorter et al. 2016).

We right censored data at 60 days or when an elk event had not occurred prior to the end of a season to meet the proportional hazard assumptions. Censored records were assigned the mean group size of all other elk observations from the corresponding season. We tested for differences in the distributions of elk revisit times across a subsample of cameras operating during both years (winter: n = 17; summer: n=28) using a Kolmogorov-Smirnov (KS) test. If distributions did not

significantly differ across years within a season, we combined data from both years rather than stratifying observations by year. Although cameras were set up at a site to maximize the field of view, this may not have had led to each site monitoring an equal-area due to the landscape features, which may have influenced elk detection and revisit times. For this reason, we used camera site as a random effect when modelling revisit times to control for detection of events at a site and because multiple events occurred each camera site.

We used a mixed effects Cox proportional hazards model (Yau 2001) to determine the influence of covariates on the relative risk of a camera site being revisited by any elk:

$$h(t) = h_0(t)exp(\beta_1 x_1 + \ldots + \beta_n x_n)$$

where $h(t)$ is the hazard at time (t), $h_0(t)$ is the unspecified baseline hazard, and β_n are the coefficients of the covariates x_n that alter the hazard of elk revisiting at any given time and the random effect was camera site because of repeated observations at the same camera. An increase in the relative risk of elk visiting a camera corresponds to a decreased time to event (*i.e.*, shorter revisit time).

We followed a 2-step process in modeling the effects of covariates. We assessed 4 metrics of seasonal elk movement rate or distribution (see below) to control for their effect on possibly varying rates of encounter with the cameras regardless of elk grouping behavior or site characteristics. First, we tested for seasonally varying movement and distribution of GPS-collared elk. Second, we tested for the effect of seasonal shifts in movement or distribution on revisit times. Where we found evidence that movements or seasonal shifts in distribution influenced revisit time, we considered these variables as part of the null model to further assess elk grouping behavior and site characteristics. We used a model selection approach based on Akaike's Information Criterion

(AIC) to select the best supported model with a conservative cut-off of ΔAIC = 4 (Burnham and Anderson, 2002). If there were competing top models (ΔAIC < 4), we removed variables where confidence intervals overlapped zero. All models were developed with the '`coxme`' function in the R survival package. Model selection was performed using the R package `MuMin` (Barton 2016). We report standardized (2 SDs) hazard ratios (HRs), allowing for beta coefficients of continuous predictors (fixed site features) to be directly comparable with untransformed binary predictors of predator presence (R package `arm`; Gelman, 2008). We used Schoenfeld residual analysis to test the assumption of the proportional hazard model (Cleves et al. 2008). Due to large sample sizes, we used $P < 0.01$ as a conservative approach for rejecting significant deviations from 0 in the slopes of fitted Schoenfeld residual curves.

Seasonal elk movements and distribution

Because elk movements and space use may vary within a season and influence revisit times independently attraction to the site, we used data from GPS-collared elk (n= 20) in 2017 to estimate temporal patterns in (i) daily movement rates (m/hr), (ii) home range sizes (km^2), and (iii) proportion of locations within the camera area during winter and summer. To estimate movement rates, we calculated mean daily 1-hr step lengths (hereafter, daily movement rates) across all elk and compared linear, quadratic, and cubic models to the seasonal average (null) in a model selection approach to account for the different model parameters. We used ΔAIC > 4 to determine which model describing movement trends best fit the data. We did not include elk movement rates as a covariate when modeling revisit times if we found no within-season trend. Where we found a within-season trend in movements, we used the model to predict daily movement rates for each day between elk events and used the averaged value for the period in the model.

To calculate seasonal trends in mean home range size and mean proportion of GPS locations (hereafter, proportions of locations), we divided winter equally into an early (1 Dec – Jan 20), middle (21 Jan – 11 Mar), and late period (12 Mar – 30 Apr) and summer into very early (1 June – 25 June), early (26 June – 25 July), midsummer (26 July – 24 Aug), and late summer (25 Aug – 15 Sept). Very early summer represented the calf-rearing period, which began on the median parturition date of resident elk (May 30) and ended after 26 days, when post-calving increases in movements and daily home range size have been shown to reach an asymptote (Berg 2019). The remaining periods were delineated based on expected changes in movement rates, with early and midsummer periods encompassing all movement rates above the seasonal average, and late summer including those below. Each period included a nearly equal number of days (18 – 21 days). Every day within a period was assigned the mean value for elk home range size and proportion of locations, which resulted in a weighted average being calculated across the time between elk events used in modelling revisit times. We assumed seasonal variation in movements and space use was similar among years and applied any temporal trends found in 2017 across elk observations in 2018 because we did not have similar data for elk in 2018 (*i.e.*, fix rates > 2 hrs). We used a Kruskal–Wallis test to determine if the proportion of locations in the camera area and home range sizes were significantly different across any of the within-season periods and report significant differences between specific periods using Wilcoxon Signed-Rank tests with a Bonferroni Correction. For metrics of movement and space use that significantly differed across periods, we used model selection to test which metric best predicted (ΔAIC > 4) elk revisit times in the absence of any other covariates.

Elk group characteristics and predator occurrence

Elk group size was measured as a continuous variable and estimated from the full sequence of photographs for each event. Herd counts began on the first image of an event and elk moving into the frame were added as they appeared. If the herd was moving in a single direction, only individuals entering the frame in that direction were counted. Individuals moving in the opposite direction were only counted if we confirmed they were not a previously counted individual circling back into view (via marked collars, tag IDs, or other distinguishing features). When large groups were present, we limited group size to the maximum herd count estimated from 95% of all other elk observations in each season (Appendix 3). Presence of at least one calf was also recorded for groups. Events were classified as a bachelor herd only if all observed elk were branched antlered bulls. Photographs of predators (wolves, grizzlies, and cougars) and humans were subject to the same protocol as elk, with human events including both hikers and horseback riders. The occurrence of predators between elk events was entered into models as a categorical covariate (present or absent) for each predator species in efforts to reduce the sampling bias associated with longer revisit times. The presence of any predator between elk events, regardless of species, was also included to test whether revisit times were influenced by each predator equally.

Camera site characteristics

Fixed-effect site characteristics included the proportion of nearby vegetation types, terrain ruggedness, density of forest edges, and proximity to different sources of human activity and other natural features (*e.g.* major creeks and the Red Deer River; Table 2). Vegetation types were derived from TM Landsat imagery by collapsing 16 landcover classifications into 6 generalized vegetation types, including conifer, deciduous-mixed, forest regenerated vegetation, herbaceous, shrub, and burned areas (Hebblewhite, 2006). Proportion of nearby vegetation types and linear densities of

forest edges and recreational horse trails (km/km^2) were calculated within a 300-m buffer around each camera location. The potential influence of ranch activities was measured as the nearest linear distance of each camera to the ranch buildings and to the main gravel road. Terrain ruggedness was derived from a digital elevation model (DEM). Any fixed site characteristics correlated with a Pearson correlation (*r)* > |0.50| were not included in the same model. Correlations between fixed site characteristics across cameras were assessed independently for both winter and summer, as elk did not occur on all the same cameras across seasons.

RESULTS

Image classification summary

Elk were detected at 36 of 44 remote cameras in winter and 44 of 44 cameras in summer, with a total of 418 elk events in winter and 877 in summer (Appendix 2). Of these, 64% (n = 266) were >12 hrs apart during winter and 76% (n = 665) were >12 hrs during summer. Distribution of elk group sizes in winter differed from those in summer (KS test, $D = 0.41$, $P < 0.001$), with a median group size of 8 in winter (14.8 ± 1.4 [mean ± SE], 95% < 60) and 2 in summer (4.8 ± 0.4, 95% < 20; Appendix 3). In winter, 57 elk events (21%) were bachelor herds. During summer, 83 elk events (12%) were bachelor herds and 117 events (18%) had at least one calf present.

Wolf events in winter (n = 97) occurred at 42 % (n = 16) of the cameras in 2017 and 32% (n = 12) in 2018. Wolves co-occurred with elk at 24 cameras across both winters and were present between elk events on 24 occasions (n = 50 events). In summer, wolf events (n = 98) occurred at 11 (30%) cameras in 2017 and 17 (38%) cameras in 2018, with wolves detected at 7 of these locations in both summers. This resulted in 52 occasions (n =85 events) at 19 camera sites when wolves were present between elk events in summer. Grizzly bear events (n = 68) occurred at 9

(25%) cameras in 2017, 18 (41%) in 2018, and at 5 of the same cameras across years during summer. Grizzlies were detected between elk events on 38 occasions at 22 camera sites (n = 54 events). No black bears were detected during the study period. Cougar events during summer (n = 16) were distributed across 15 locations, resulting in 9 occasions when cougars were detected between elk events (Appendix 2). Cougars co-occurred at cameras with elk only during winter in 2018 (n = 4 locations; 1 event/location) and were excluded from analysis.

Seasonal elk movements and distribution

Winter — Mean daily movement rate [± SE] of GPS-collared elk in winter was 139.39 ± 7 m/hr. Daily movement rates of elk in winter were best predicted by the null model indicating no within-season trend in elk movements (Table 3, Fig 3). Nearly all (99%) of the winter GPS elk locations in occurred within the study area indicating elk were similarly exposed to cameras across the winter. Mean home range sizes showed a small but significant increase from the early (23.4 ± 1.1 km^2) to middle (25.1 ± 0.8 km^2) winter periods (t = –5.76 , df = 38, P <0.001), and a decrease in home range size in the late period (13.5 ± 2.0 km^2) compared to the early (t = 19.83 , df = 38, P <0.001) and middle periods (t = 24.6 , df = 38, P < 0.001). As a result, only home range size was assessed in time-to-event models to control for changing exposure to the camera area in winter.

Summer — Daily movement rates of GPS-collared elk were significantly higher in summer than in winter, with a mean of 233 ± 9 m/hr (t = –15.9, df = 233, P < 0.001). Seasonal variation in daily movement rates was best supported by a quadratic function (Table 3), with movement rates increasing steadily from the start of the summer period until 25 July before decreasing until 15 September (Fig. 3). There was a significant difference between the mean proportion of locations within the camera area throughout the four summer periods (Kruskal-Wallis (KW) test; χ^2 = 17.4, df = 3, P < 0.001; Fig. 4). The proportion of locations during the very early period (*i.e.*, calving;

85%) was significantly higher than the early (65%, $P = 0.003$), middle (65%, $P = 0.004$), and late periods (69%, $P = 0.012$, Appendix 4). The proportion of locations in the early, middle, and late periods were not significantly different ($P > 0.99$). Home range size significantly differed across the four summer periods (KW test; $\chi^2 = 44.6$, $df = 3$, $P < 0.001$; Fig. 4). Mean home ranges in very early summer (26 ± 3.5 km^2) were significantly smaller than those in early (68 ± 4.1 km^2 ($P <$ 0.001) and middle summer periods (68 ± 4.6 km^2, $P <$0.001). Home range sizes during very early and late summer (34 ± 3.3 km^2) were the not significantly different ($P = 0.25$), as were the early and middle periods ($P > 0.99$). All metrics of elk movements and distribution were highly correlated ($r = 0.68 – 0.86$) and could not be included in the same models (Appendix 5).

Modelling elk revisit times

Distributions of revisit times did not differ between years within a season for cameras sites used in the same years ($n_{Winter} = 17$; $n_{Summer} = 28$, KS test, $P_{Winter} = 0.14$, $P_{Summer} = 0.11$; Appendix 6, 7). Elk had median revisit time in winter of 8 days (14.3 ± 1.0 [mean ± SE]; n = 266), which was longer than the median revisit time of 2 days in summer (9.7 ± 0.6; n = 665). Using a 60-day revisit threshold for right censoring elk revisit times, removed only 5.3% (n = 14) elk revisit times in winter and 1.6% (n = 11) in summer, but allowed us to meet the assumptions of the Cox proportional hazard model in all the models presented ($P < 0.02$; Appendix 8). Although a substantial proportion of revisit times were below the threshold of 12 hrs and excluded from the analysis presented here (36% in winter; 24% in summer), we explored different cut-off times and found betas among candidate models varied minimally (overlapping 95% CI) when including revisit times <12 hrs. Across camera sites, distance to the main road was positively correlated with distance to the ranch buildings ($r = 0.68$, $P < 0.001$) and edge density within a 300-m buffer ($r =$ 0.59, $P < 0.001$); Appendix 9). Edge density was also correlated with proportion of open habitat

within a 300-m buffer (r = 0.56, P <0.001), and as a result, these variables were not used in the same models.

Winter — Despite changes in home range sizes during winter, home range size across winter did not improve the model fit over the null model (ΔAIC < 1, Table 4), and, therefore, was not included further in model evaluations. Three top models predicting revisit times of elk had equal support (ΔAIC < 2) and included proportion of grasslands, wolf occurrence, and either an interaction between proportion of grasslands and wolf occurrence or distance to road (Table 5). Based on the hazard ratio, elk revisited 61% sooner to sites that had a high proportion of surrounding grasslands, took 68% longer to revisit when wolves occurred, but the delay was less (wolf × grassland interaction) when sites were surrounded by grassland (Table 6; Fig. 5). Revisit times to a site were consistently longer when wolves had been detected between elk events, with the greatest effect in the first 15 days (Fig. 6). Revisit times were 12% longer with increasing distance to a gravel road (Table 7). Global tests of non-zero slopes in Schoenfeld residuals were nonsignificant for candidate models, suggesting the data did not violate the proportional hazards assumption. Plots of scaled Schoenfeld residuals from each covariate in the top model (P_{Global} = 0.16) across time showed minimal variation in predicted beta values throughout the winter study period (P = 0.06 – 0.60; Appendix 10).

Summer — Of the movement and distribution metrics in summer, proportion of locations within the camera area was better supported in predicting elk revisit times than other metrics (ΔAIC > 25, Table 6) and than the null model (ΔAIC = 59.97). As a result, we included this metric in all candidate models to account for shifts in elk distribution and lower density of elk in the camera area over the summer. The most supported models predicting revisit times in summer consistently included at least one previous visit by each predator species rather than counts of predator events,

with the best supported model also including density of nearby edges (Table 7). Elk revisit times to sites surrounded by higher edge densities were 12% longer (Table 6, Fig. 7). Revisit times of elk to a site where a predator had previously occurred increased by 57% (HR = 0.43 , CI = 0.30–0.60) when the predator was a wolf, 40% (HR =0.6, CI = 0.41–0.87) when it was a bear, and 66% (CI = 0.14–0.85%) when it was a cougar (Fig. 6). Models that included a covariate for whether any predator, regardless of species, occurred between elk events were not well supported (ΔAIC > 6). There also was moderate support (ΔAIC = 2.03) for shorter revisit times as elk group sizes increased (Fig. 7). There was not sufficient support (ΔAIC > 4) for any interactions between predator presence and group size or edge density, or for any metrics related to human activity influencing revisit times in summer. Schoenfeld residual curves showed no trends in the plotted residuals for each covariate used in the top model ($P_{\text{Global}} = 0.02$), which is further supported by the corresponding Grambsch–Therneau tests ($P = 0.02–0.99$; Appendix 11). Visual inspection of residuals for wolf and grizzly presence reveals they are symmetric about 0 until approximately 20 days (t = 15–31 days), when a predator's influence on elk revisit times might be expected to decrease.

DISCUSSION

Elk were observed at most camera sites across the Ya Ha Tinda in both seasons. The number of elk events at cameras and the distribution of revisit times did not differ between years at the same sites, which was expected because the elk population size and migratory patterns did not show major changes during the study period (Berg 2019). Despite a decrease in the proportion of locations within the camera grid in summer by migratory elk (Eggeman et al. 2016), the number of events at camera sites in summer increased and median revisit time in summer was almost four times that of winter. The increase was related to a 60% increase in elk movement rates as well as

well as smaller aggregations, with group sizes averaging only about 33% of those in winter. in Smaller group sizes and faster movement rates, that have been reported for elk previously (Jedrzejewski et al. 2006, Hebblewhite and Merrill 2011, Rossatte 2016, Brennan et al. 2015), represented an important mechanism governing revisit times.—We also hypothesized that elk numbers and distribution at the Ya Ha Tinda would influence encounter rates with cameras and the baseline revisit times as indicated in other uses of camera data, such as estimating animal density (Rowcliffe et al. 2008, Burton et al. 2015, Lucas et al. 2015, Moeller et al. 2018). Indeed, ancillary data on individual animals' movements within a sampling grid has also been incorporated into estimating density with spatial capture-recapture (Royale et al. 2013). This hypothesis was supported in summer (H_2; mean proportion of relocations in the camera grid), but not in winter. In summer, the shift in elk use of the Ya Ha Tinda in early- and mid-summer was large enough to differentiate revisit times from those in very early and late summer. High use of the camera area by resident elk in very early summer may have reflected isolation during calving when elk have been found to reduce the size of the area used for ~26 days after calves are born (Berg 2016). Reasons for high use of the camera grid in late summer by resident elk is less clear but may be related to a period when forage maturation offers fewer opportunities to find high quality patches and increased use the Ya Ha Tinda, when human activity is still relatively high and provides a refuge from predation (Hebblewhite and Merrill 2009). Although we used proportion of points within the camera grid to reflect changes elk encounter rates with cameras in summer, we also found support for revisit times being influenced by both home range size and movement rates. Because estimates of movement rates, home range size, and proportion of GPS locations were correlated, we were unable to assess additive effects of elk movements and shifting distributions except as ratio of one metric to another. Because we found less support for this ratio than for shifts

in GPS-collared elk use of the area, we suggest shifts in elk distribution had the greatest effect on the baseline encounter rates with cameras in summer.

We avoided confounding the seasonal effects of these shifts in distribution and movement behavior by modeling revisit times by season. In winter, we found the extent of grassland around the camera site increased and the occurrence of a wolf delayed revisit times of elk to a site. These results are consistent with selection patterns of individual GPS-collared resident elk at the Ya Ha Tinda (Killeen et al. in prep). They found resident elk consistently selected for forage abundance, which is highest in grasslands (Hebblewhite 2006), and avoided risky areas due to wolves, with evidence for a similar trade-off where elk selected against high forage areas in wolf-risky areas. While we were unable to include cougars in winter models due to their limited co-occurrence with elk on cameras during only one year of the study (4 locations; 1 event/location), we might expect cougars to pose a limited threat to elk in winter for this system, as research in the adjacent Banff National Park has shown cougars prey-switching in winter from elk to deer in response to recolonizing wolves (Kortello et al, 2007). In the presence of predators, particularly wolves in winter, elk may also select open habitats because they provide visibility of predators that allows for early escape (Profit et al. 2015, Brennan et al. 2015). For example, Hebblewhite et al. (2005) found that in open grasslands the risk of an elk encountering a wolf was high, but the risk of being killed by a wolf after being encountered was lower than in forests.

Alternatively, Robinson et al. (2010) also reported that during the day, wolf intensity of use was concentrated around the periphery of the grasslands within the surrounding timber (Fig. 1; see photograph) resulting in relatively low predation risk on the grasslands except along the edge of forests. We did not find that edges, where wolves are known to hunt and successfully kill elk (McPhee et al, 2012; Bergman et al, 2006), was a better predictor of revisit times in winter than

the direct occurrence of a wolf, but we did find that wolves were observed more frequently at cameras located on forest edges (63%) than in the grassland (37%). In contrast to summer, elk may not avoid using areas near edges in winter especially if easily-accessible (*i.e.* snow free) forage is depleted elsewhere and may only use predator presence as a direct cue for imminent predation risk (Liley and Creel 2008). Further, the distinct daily pattern of wolf use of the Ya Ha Tinda, which is attributed to wolf avoidance of high human activity during the day (Hebblewhite and Merrill 2008), may contribute, in part, to the trade-off (*i.e.*, interaction) we found between forage and predation in the model of winter revisit times models if elk avoid risky areas at night. Although we cannot evaluate daily patterns with the presented framework of revisit times, elk observations on cameras were more frequent during the day (64%) and wolves at night (73%). In summer when resources were less limiting, we found that revisit times most closely reflected direct and indirect predation risk (H_6 and H_7) rather than attraction to vegetation types. After accounting for shifts in proportion of locations within the camera grid, elk revisit times were influenced to different extents by the occurrence of each major predator species. Models that did not distinguish between which predator species was present performed poorly ($\Delta AIC > 6$) in comparison to those that included each predator separately, given prey vulnerability to predation is dependent on each predator's hunting mode (Christianson et al. 2018; Lone et al. 2014; Thaker et al. 2011), territory size and prey management (Schlagel et al. 2017), and can vary seasonally (Metz et al. 2018; Griffin et al. 2011). We found additional evidence that elk also responded to the indirect threat of predation by avoiding areas of high edge density. We also found minimal support for group size influencing revisit times in winter, which may be driven by limited variation among larger group sizes on the winter range, often consisting of more than 200 individuals (Killeen, in prep). It is also possible that remote cameras did not provide reliable estimates of group size, as 95% of all events

contained ≤ 60 elk (with the remainder ranging from only 83 to 144). However, given we found revisit times of larger groups decreased in summer, grouping dynamics when group sizes are smaller may a play a key role in antipredator behavior that may not only dilute predation risk (Gower et al. 2009; Fortin and Fortin 2009, Proffitt et al. 2008; Hebblewhite and Pletscher 2002), but also improve the efficiency in using the landscape under high predation risk (Gude et al. 2006, Eisenberg et al. 2014).

Because we could not distinguish between individual elk captured on cameras, revisit times are a result from repeated observations of the same elk or different groups, rather than actual return time of an elk that has visited the site previously (Berger-Tal and Bar-David 2015). Nevertheless, frequency of use by elk, which we quantified as revisit times, reflects the attractiveness of the site and the variation in visitation rates may reflect the predictability of elk being at the site (Bowyer et al. 1999, Anderson et al. 2008). In our study, elk revisitation of a site was most influence by resources when they were most limiting (*i.e.*, winter), whereas risky places were revisited less often year-round. We found little support in either season that human activity (H_8 & H_9) influenced elk visitation of a site, which is likely because resident elk are habituated to humans (Robinson and Merrill 2013). On the other hand, we found that risky places because of predators (H_6 & H_7) were revisited less often and that there was a seasonal effect on whether direct or indirect cues of predators influenced revisitation rates, elk showing a conservative approach to using indirect cues only when resources were abundant. Our study implicates a prey's perception of predation risk and the precautionary behaviours that follow can be initiated long before a predator is directly encountered (Latombe et al. 2014; Profitt et al. 2009; Creel et al. 2005). Proactive risk avoidance requires at least some components of risk to be predictable that can be developed through learning and memory (Creel 2018), but short and long-term behavior decisions in using risky place may be

shaped by trade-offs in selecting for resources when they are limited. Using data from remote cameras that permit quantification of revisit frequency and its variation offers an opportunity to advance our understanding of behavioral dynamics of prey space-use particularly at the small scale.

Table 1. Hypotheses and predictions of the effects of movements, site preferences, predation risk, and reproductive status on revisit times of non-migratory elk to camera sites in the Ya Ha Tinda range along the east slope of the Rocky Mountains, Alberta.

	Concept	Prediction	Variables	Effect direction
Baseline exposure hypotheses				
H_1	Elk home range size	Large home range size of elk increases revisit time.	Mean seasonal MCP of GPS-collared elk	+
H_2	Elk distribution	High overlap of elk using the camera grid shortens revisit time.	Mean seasonal percent of locations of GPS-collared elk in camera area	–
H_3	Random encounter	Longer seasonal movements shorten revisit time.	Mean 2-hr step lengths of GPS-collared elk	–
H_4	Movement/home range area	Higher ratio of movements to home range shortens revisit time.	Home range and movement rates of GPS collared elk (as above)	–
Ecological hypotheses				
H_5	Preference for site characters	Elk revisit time is shorter to preferred sites.	Site characteristics: land cover, forage, water	–
H_6	Direct predator avoidance	Elk revisit time is longer after predator(s) observed at camera site.	Wolf, bear, cougar or any of the predators observed at camera site	–
H_7	Indirect predator avoidance	Elk revisit time is longer at cameras adjacent to forest edge	Forest edge density	–
H_8	Human refuge from predators	Elk revisit time is shorter to areas of high human use due to predator avoidance	Distance to trails, ranch infra-structure; hikers/horse riders observed on camera	+
H_9	Human avoidance	Elk revisit is longer to areas of high human use due to predator avoidance	Distance to trails, ranch infra-structure, main road	–
H_{10}	Group size dilution	Elk revisit time after predator or near edge shortens as group increases	Interaction between predators and group size	+
H_{11}	Calf present	Elk revisit time after predator or near edge increases with when calf present	Occurrence and number of calves/cow present interaction with predators	+

Table 2. Covariates used for modelling elk revisit times with photographs of elk and their predators collected at remote cameras across the winter range of the Ya Ha Tinda, along the eastern slopes of the Rocky Mountains of Alberta, Canada. If data sources are not indicated (--), covariates were created by the authors with project data.

Variable	Code	Data description	Units	Source	Year
Daily movement rate	Movements	Mean daily movement rate calculated across the time between each pair of elk events	m/2 hr	--	2017
Proportion of points	Prop.pts	Mean proportion of locations of GPS-collared elk contained within the study area (MCP) during defined seasonal periods	%	--	2017
Home range size	Home.range	Mean home range size of GPS-collared elk during defined seasonal periods	km^2	--	2017
Elk group size	Group.size	Total number of elk estimated from photographs	1,2,3…	--	2017/18
Calf presence	Calves	Whether calves were detected	0/1	--	2017/18
Bachelor herd	Bulls	Whether the revisiting elk event had only adult bull elk	0/1	--	2017/18
Wolf presence	Wolf	Whether wolves occurred (1) between elk events or were absent (0)	0/1	--	2017/18
Wolf count	Wolves	Number of wolf events between elk events	1,2,3…	--	2017/18
Grizzly presence	Grizzly	Whether grizzly bears occurred between elk events or were absent	0/1	--	2017/18
Grizzly count	Grizzlies	Number of grizzly events between elk events	1,2,3…	--	2017/18
Cougar presence	Cougar	Whether cougars occurred between elk events or were absent	0/1	--	2017/18
Cougar count	Cougars	Number of cougar events between elk events	---	--	2017/18
Predator presence	Predator	Whether any predator species occurred between elk events	1,2,3…	--	2017/18
Grassland	Grassland	Proportion of grassland landcover within a 300-m buffer	%	TM Landsat imagery	2009
Open canopy areas	Open	Proportion of grassland, herbaceous, and burned landcover types within a 300-m buffer	%	TM Landsat imagery	2009
Closed canopy forest	Closed	Proportion of conifer, mixed, and deciduous forest landcover within a 300-m buffer	%	TM Landsat imagery	2009
Distance to ranch	Dist.ranch	Distance to perimeter fencing around the ranch buildings	km	--	2018
Distance to road	Dist.road	Distance to main gravel road	km	--	2018
Distance to water	Dist.water	Distance to nearest major waterway, including Scalp Creek, Bighorn Creek, and the Red Deer River	km	AltaLIS	1996
Distance to nearest edge	Dist.edge	Distance to nearest edge, where edge is the interface of open canopy areas with conifer or mixed/deciduous forest	km	Derived from TM Landsat imagery	2009
Edge density	Edge.dens	Linear density of edge within a 300-m buffer	km/km^2	Derived from TM Landsat imagery	2009

Trail density	Trail.dens	Linear density of non-motorized human/horse trails within a 300-m buffer	km/km^2	AltaLIS	2014
Elevation	Elev	digital elevation model (DEM 30; 730−3737 m)	m	Derived from AltaLIS 20K Digital Elevation Model (DEM)	2009
Ruggedness	Rugged	Mean SD of elevation of 8 neighboring cells within a buffered area standardized between 0 and 1	0–1	Derived from AltaLIS 20K Digital Elevation Model (DEM)	2009

Table 3. Summary of model selection results based on AIC for predicting daily movement rates of GPS-collared elk (metres/2 hr) in winter and summer of 2017. Top models are shown in bold.

Model	**k**	**AIC**	**ΔAIC**	**AIC Wt.**
		Winter		
Null (seasonal average)	**2**	**1798.21**	**0**	**0.59**
Linear	3	1800.28	2.07	0.21
Quadratic	4	1800.93	2.72	0.15
Cubic	5	1803.07	4.86	0.05
		Summer		
Quadratic	**4**	**1270.92**	**0**	**0.70**
Cubic	5	1272.66	1.74	0.29
Null (seasonal average)	2	1285.48	14.56	< 0.001
Linear	3	1287.41	16.49	< 0.001

Table 4. Model selection results based on AIC for predicting revisit times with a single metric related to elk movements or space use in winter and summer. All models include a random effect for location ID.

Model	k	AIC	ΔAIC	AIC Wt.
		Winter		
Home.range	2	2095.55	0	0.56
Location ID (null)	1	2096.13	0.58	0.44
		Summer		
Prop.pts	**2**	**6557.54**	**0.00**	**0.99**
Movements/prop.pts	2	6583.08	25.54	< 0.001
Movements/home.range	2	6588.44	30.89	< 0.001
Home.range	2	6600.35	42.81	< 0.001
Movements	2	6607.32	49.78	< 0.001
Location ID (null)	1	6617.51	59.97	< 0.001

Table 5. Model selection results based on AIC for predicting revisit times of elk at remote camera sites across the Ya Ha Tinda during winter (1-December to 30-April). All models include a random effect for location ID. The top models are shown in bold. See variable definitions in Table 2 and all other candidate models tested in Appendix 11.

Model	k	AIC	ΔAIC	AIC Wt.
Wolf + grassland	**3**	**2066.79**	**0**	**0.44**
Wolf + grassland + dist.road	**4**	**2068.03**	**1.25**	**0.23**
Wolf + grassland + wolf×grassland	**4**	**2068.53**	**1.74**	**0.18**
Wolf + grassland + edge.dens	4	2068.83	2.04	0.16
Wolf + grassland + group.size	4	2068.83	2.05	0.16
Wolf + grassland + dist.road + wolf×dist.road	5	2068.85	2.07	0.15
Wolf + grassland + dist.road + wolf×grassland	5	2069.90	3.11	0.092
Wolf + grassland + dist.road + group.size	5	2070.05	3.27	0.085
Wolf + grassland + herd size + wolf×herdsize	5	2070.43	3.64	0.071
Wolf + grassland + herd size + wolf×grassland	5	2070.59	3.81	0.065
Wolf + grassland + dist.road+ group.size + wolf×group.size	6	2071.58	4.79	0.040
Location ID (null)	2	2096.09	29.30	< 0.001

Table 6. Beta coefficients (± SE) and hazard ratios (HR ± CI [95%]) of the best models predicting revisit times of elk at remote cameras during winter and summer across the Ya Ha Tinda ranch property (2017–2018). Both models include location ID as a random effect. Hazard ratios with values >1 indicate a *decrease* in revisit times (of 1–HR) and those with values <1 indicate an *increase* in revisit times. For example, the presence of wolves increases revisit times by 68% during winter (1 – 0.32 = 0.68).

	Winter			**Summer**		
	β ± SE	**HR**	**CI (95%)**	**β ± SE**	**HR**	**CI (95%)**
Prop.pts	--	--	--	0.37 ± 0.05	1.45	1.33 – 1.59
Grassland	0.46 ± 0.08	1.61	1.35 – 1.87	--	--	--
Edge density	--	--	--	–0.11 ± 0.06	0.89	0.78 – 1.01
Elk group size	–	--	--	0.007 ± 0.05	1.01	0.92 – 1.10
Wolf presence						
× Grassland	–0.25 ± 0.40	0.78	0.40 – 1.70	--	---	--
Wolf presence	–1.02 ± 0.30	0.32	0.20 – 0.65	–0.85 ± 0.17	0.43	0.30 – 0.60
Grizzly presence	--	--	--	–0.51 ± 0.19	0.60	0.41 – 0.87
Cougar presence	--	--	--	–1.07 ± 0.47	0.34	0.14 – 0.85

Table 7. Summary of model selection results based on AIC for predicting revisit times of elk at remote camera sites across the Ya Ha Tinda during summer (1-June to 15-Sept). All models include a random effect for location ID. Top model is shown in bold. See all other candidate models tested in Appendix 12.

Model	**k**	**AIC**	**ΔAIC**	**AIC Wt.**
Prop.pts + wolf + grizzly + cougar + edge.dens	**6**	**6514.02**	**0**	**0.44**
Prop.pts + wolf + grizzly + cougar + edge.dens + group.size	7	6516.05	2.03	0.16
Prop.pts + wolf + grizzly + cougar + dist.road	6	6516.49	2.47	0.13
Prop.pts + wolf + grizzly + cougar + group.size	6	6517.09	3.07	0.094
Prop.pts + wolf + grizzly + cougar + group.size + dist.ranch	7	6517.79	3.77	0.066
Prop.pts + wolf + grizzly + cougar + edge.dens + group.size + group.size×edge.dens	8	6518.10	4.08	0.057
Prop.pts + wolf + grizzly + cougar + group.size + dist.road	7	6518.45	4.43	0.048
Prop.pts + edge.dens + group.size + predpres	5	6520.87	6.86	0.014
Prop.pts	2	6557.541	43.52	< 0.001

Figure 1. The winter range of Ya Ha Tinda, with an impressive view into Banff National Park. Photographed by Jacalyn Normandeau.

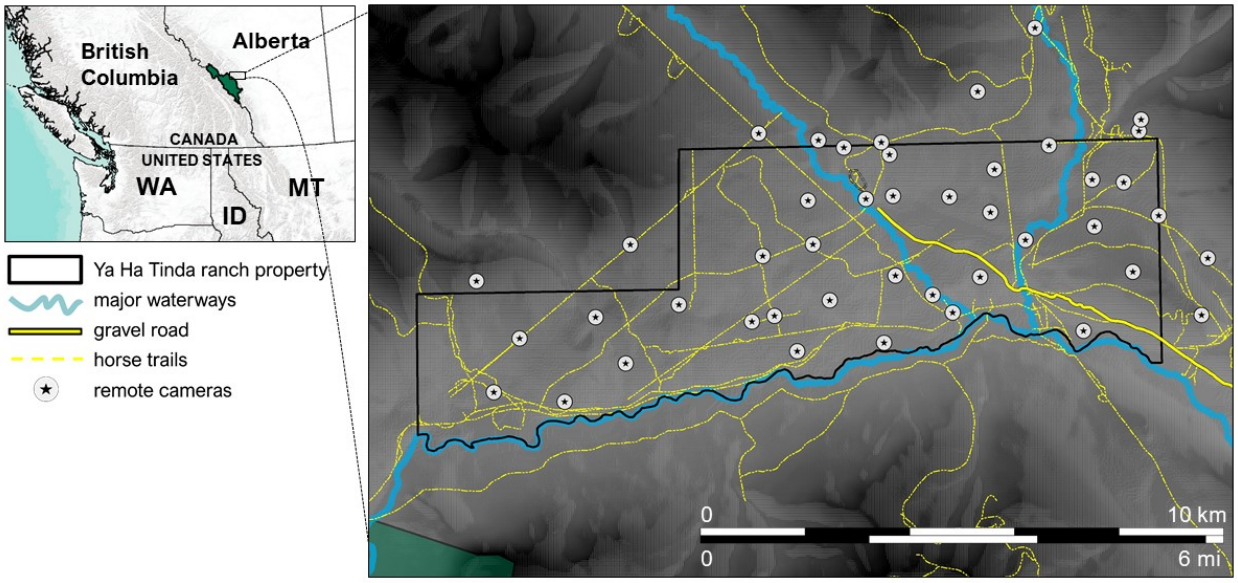

Figure 2. Distribution of remote cameras (n = 44) across the winter range of the Ya Ha Tinda's partially migratory elk herd, along the eastern slopes of the Rocky Mountains, Alberta, Canada. Cameras were distributed within the minimum convex polygon of pooled 2-hr relocations of GPS-collared elk (n = 20/year) from the winters of 2010 to 2015.

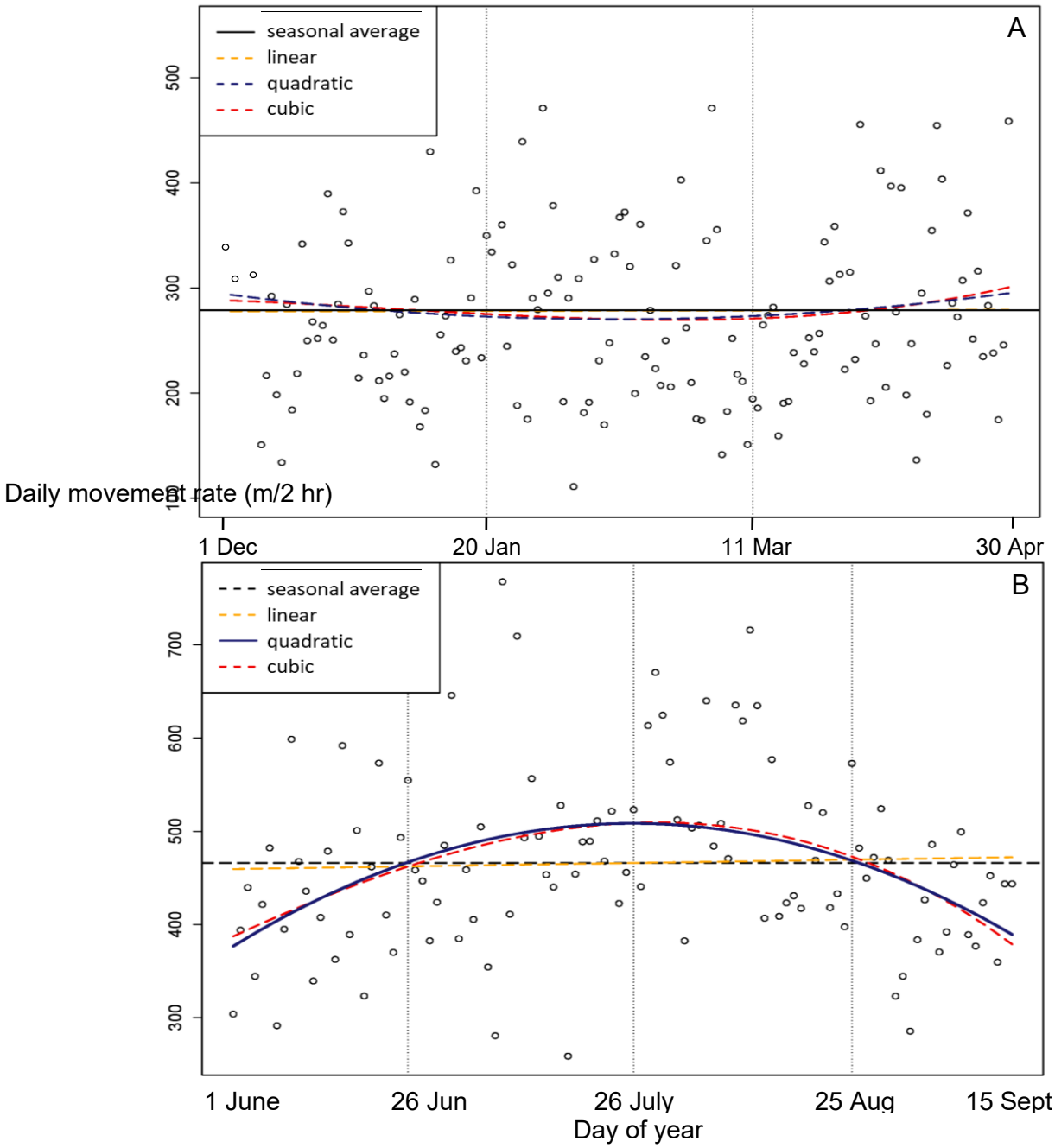

Figure 3. Mean daily movement rates (m/2 hr) of GPS-collared elk (n = 20) fitted with linear, quadratic, and cubic functions from (A) 1 December to 30 April 2017 and (B) 1 June to 17 September 2017. Winter data was best fit by the null model (*i.e.*, seasonal average), indicating no seasonal trend (ΔAIC > 2; Table 3). As a result, daily movement rates were not included as a covariate when modelling revisit times in winter. Summer data was best fit by the quadratic model (ΔAIC > 14; Table 3). Values predicted by the quadratic model were then used for determining the average daily movement rate between elk observations used to model revisit times in summer. Top models for each season are shown with solid lines.

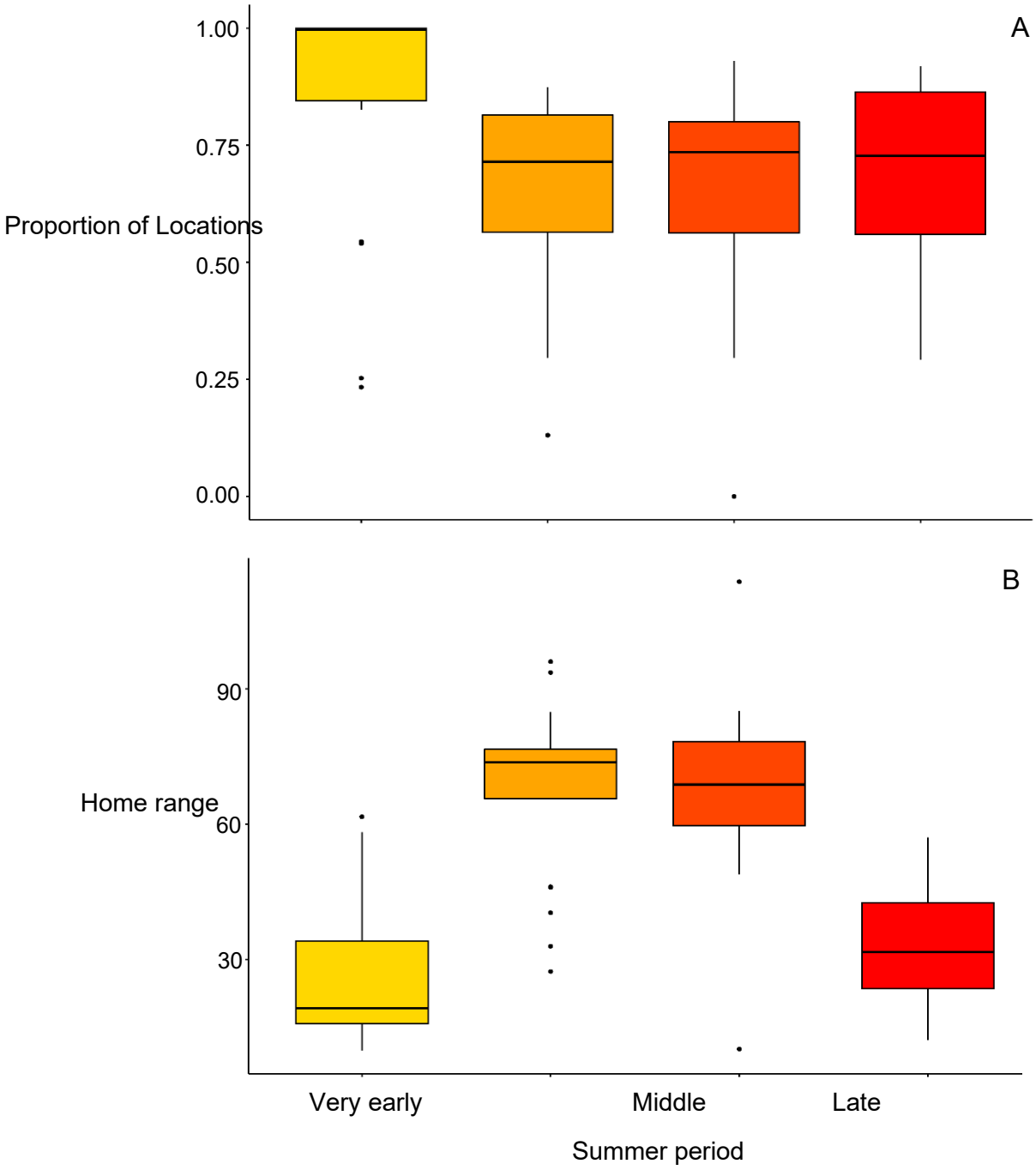

Figure 4. (A) Proportion of 2-hr relocations of GPS-collared elk (n =21) within the camera area and (B) summer home range sizes (km^2) of GPS-collared elk (n =21) across the very early (*i.e.*, calf-rearing; 1 June – 25 June;), early (26 June – 25 July), middle (26 July – Aug 24), and late summer (25 Aug – 15 Sept) periods. To view the geographical distributions of GPS relocations and home ranges across summer periods, refer to Appendix 14.

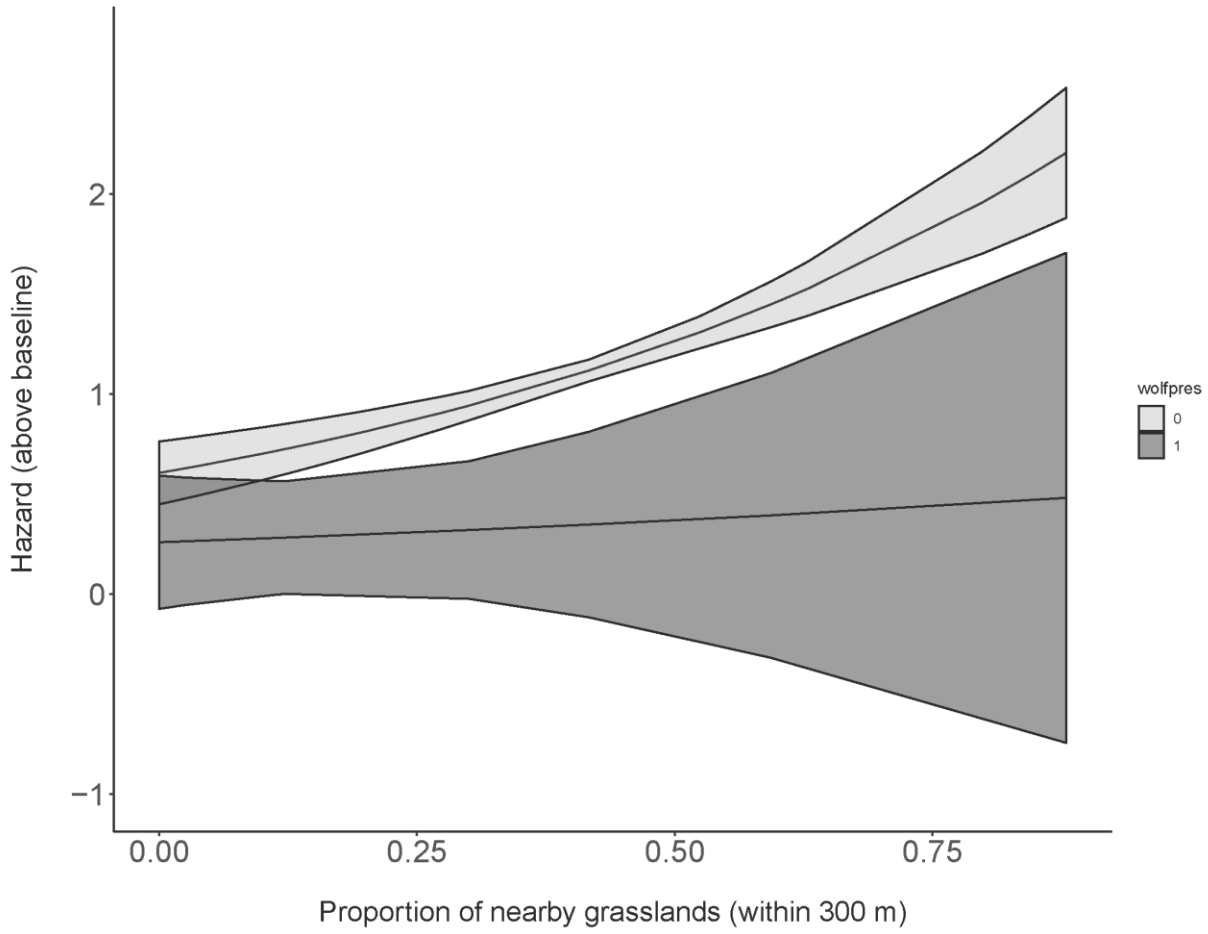

Figure 5. Hazard (or likelihood) of any elk revisiting a camera site in winter with respect to the proportion of nearby grasslands, interacted with wolves being present (1) or absent (0). Shaded regions represent 95% confidence limits.

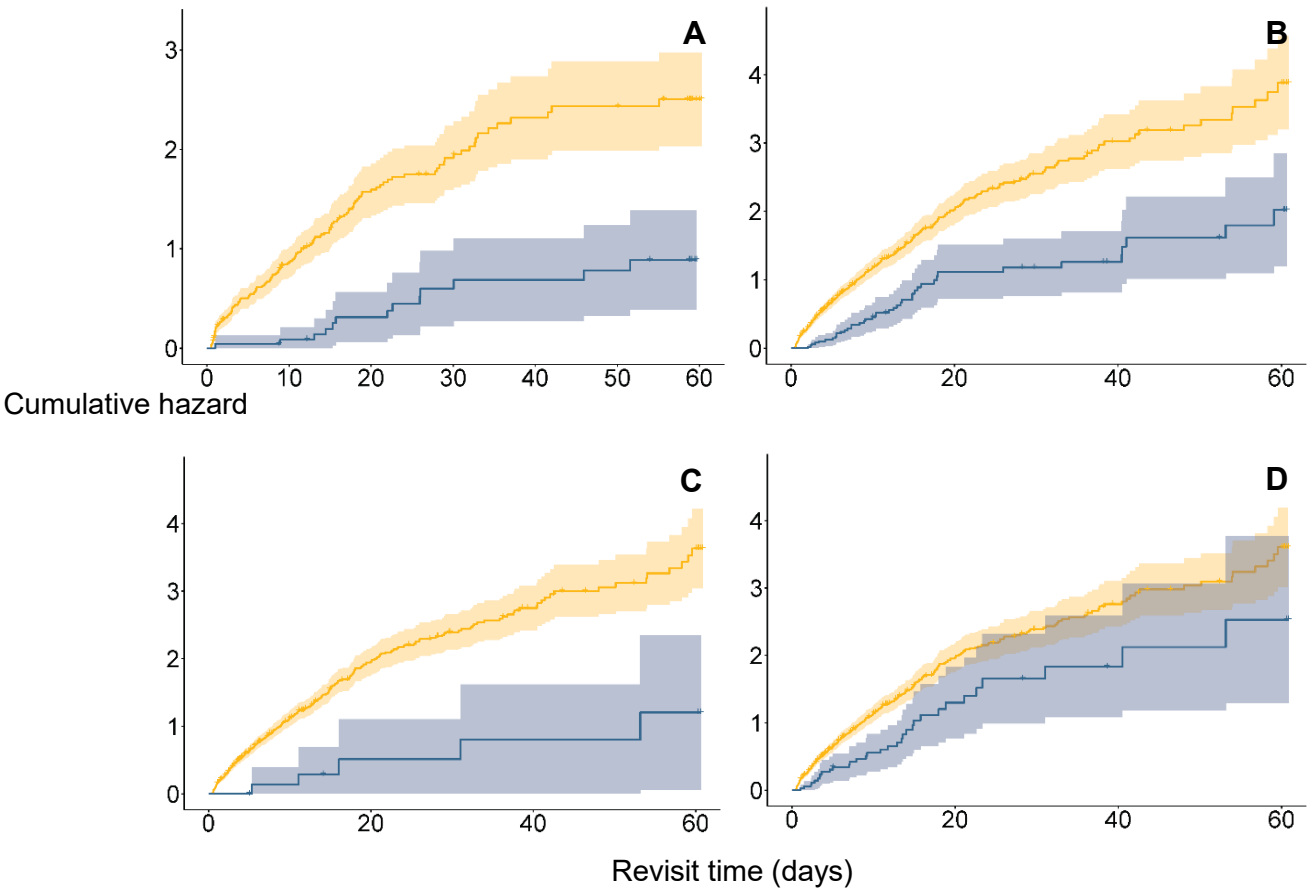

Figure 6. Cumulative hazard curves and 95% confidence limits for any elk revisiting a camera site in (A) winter when a wolf was observed (blue) or not observed (orange) between elk events or in summer when a wolf (B), cougar (C) and (D) bear was observed (blue) or not observed (orange) between elk events.

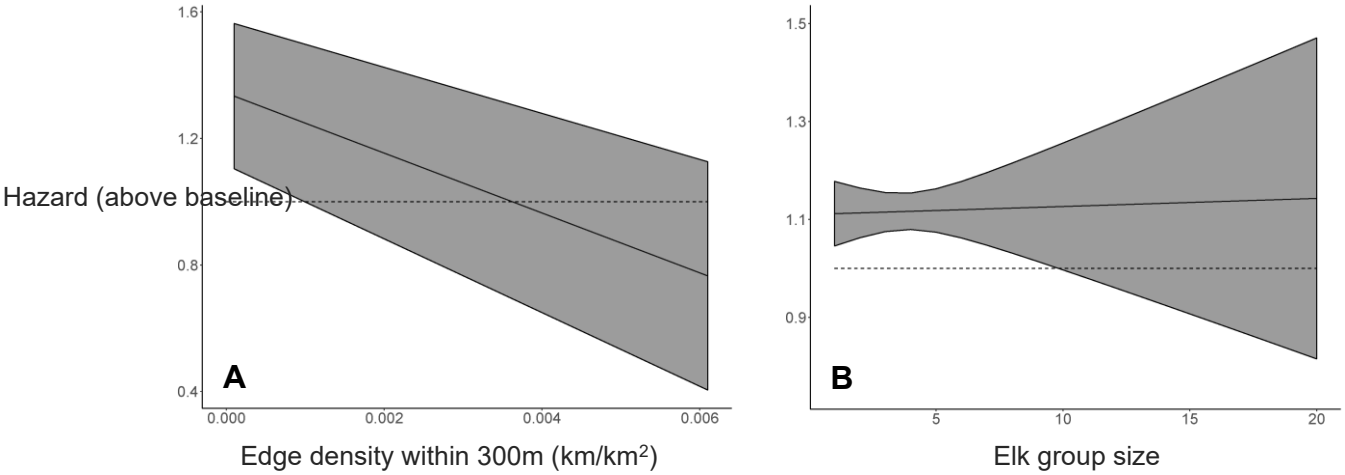

Figure 7. Hazard (or likelihood) of any elk revisiting a camera site in summer with respect to (A) increasing edge densities and (B) larger group sizes with 95% confidence limits (shaded regions). The baseline hazard ($y = 1$) is shown as a dashed horizontal line.

BIBLIOGRAPHY

Altendorf, K.B., J.W. Laundré, C.L. Gonzalez, and J.S. Brown. 2001. Assessing effects of predation risk on foraging behavior of mule deer. *Journal of Mammology* **82**:430-439.

Anderson, D. P., J. D. Forester, and M. G. Turner. 2008. When to slow down: elk residency rates on a heterogeneous landscape. *Journal of Mammalogy* **89**:105-114.

Atwood, T. C., E. M. Gese, and K. E. Kunkel. 2009. Spatial partitioning of predation risk in a multiple predator-multiple prey system. *The Journal of Wildlife Management* **73**:876-884.

Bar-David, S., I. Bar-David, P. C. Cross, S. J. Ryan, C. U. Knechtel, and W. M. Getz. 2009. Methods for assessing movement path recursion with application to African buffalo in South Africa. *Ecology* **90**:2467-2479.

Barraquand, F., and S. Benhamou. 2008. Animal movements in heterogeneous landscapes: identifying profitable places and homogeneous movement bouts. *Ecology* **89**:3336-3348.

Bassing, S. B., D. E. Ausband, M. S. Mitchell, P. Lukacs, A. Keever, G. Hale, and L. Waits. 2019. Stable pack abundance and distribution in a harvested wolf population. *The Journal of Wildlife Management* **83**:577-590.

Benhamou, S., and L. Riotte-Lambert. 2012. Beyond the Utilization Distribution: Identifying home range areas that are intensively exploited or repeatedly visited. *Ecological Modelling* **227**:112-116.

Berg, J. E. 2019. Shifts in strategy: Calving and calf survival in a partially migratory elk population. PhD thesis. University of Alberta, Edmonton, AB. 261 pp.

Berg, J., E. Spilker, J. Killeen, E. H. Merrill, and M. Hebblewhite. 2016. Ya Ha Tinda Elk and Predator Studies: 2015-2016 Update.

Berger-Tal, O., and S. Bar-David. 2015. Recursive movement patterns: review and synthesis across species. *Ecosphere* **6**:1-12.

Bergman, E.J., Garrott, R.A., Creel, S., Borkowski, J.J., Jaffe, R., and Watson, F.G.R. 2006. Assessment of prey vulnerability through analysis of wolf movements and kill sites. *Ecological Applications*. **16**(1): 273–284.

Bischof, R., S. Hameed, H. Ali, M. Kabir, M. Younas, K. A. Shah, J. U. Din, and M. A. Nawaz. 2014. Using time-to-event analysis to complement hierarchical methods when assessing determinants of photographic detectability during camera trapping. *Methods in Ecology and Evolution* **5**:44-53.

Bowyer, R. T., V. Van Ballenberghe, J. G. Kie, and J. A. Maier. 1999. Birth-site selection by Alaskan moose: maternal strategies for coping with a risky environment. *Journal of Mammalogy* **80**:1070-1083.

Bracis, C., K. L. Bildstein, and T. Mueller. 2018. Revisitation analysis uncovers spatio-temporal patterns in animal movement data. *Ecography* **41**:1801-1811.

Brennan, A., P. C. Cross, and S. Creel. 2015. Managing more than the mean: using quantile regression to identify factors related to large elk groups. *Journal of Applied Ecology* **52**:1656-1664.

Brown, J. S., and B. P. Kotler. 2004. Hazardous duty pay and the foraging cost of predation. *Ecology Letters* **7**:999-1014.

Buchanan, C. B., J. L. Beck, T. E. Bills, S. N. Miller. 2014. Seasonal resource selection and distributional response by elk to development of a natural gas field. *Rangeland Ecology & Management* **67**:369-379.

Burnham, K.P., and D. R. Anderson. 2002. Model Selection and Multimodel Inference: A Practical Information-Theoretic Approach (2nd ed.), Springer-Verlag, ISBN 0-387-95364.

Burton, A. C., E. Neilson, D. Moreira, A. Ladle, R. Steenweg, J. T. Fisher, E. Bayne, and S. Boutin. 2015. Wildlife camera trapping: a review and recommendations for linking surveys to ecological processes. *Journal of Applied Ecology* **52**:675-685.

Carbone, C., S. Christie, K. Conforti, T. Coulson, N. Franklin, J. R. Ginsberg, M. Griffiths, J. Holden, M. Kinnaird, R. Laidlaw, and A. Lynam. 2002. The use of photographic rates to estimate densities of cryptic mammals: response to Jennelle et al. *Animal Conservation* **5**:121-123.

Chandler, R. B., and J. A. Royle. 2013. Spatially explicit models for inference about density in unmarked or partially marked populations. *The Annals of Applied Statistics* **7**:936-954.

Charnov, E. L. 1976. Optimal foraging: The marginal value theorem. *Theoretical Population Biology* **9**:129-136.

Christianson, D., Becker, M.S., Brennan, A., Creel, S., Droge, E., M'soka, J., Mukula, T., Schuette, P. Smit, D., and F.Watson. 2018. Foraging investment in a long-lived herbivore and vulnerability to coursing and stalking predators. *Ecology and Evolution* **8**: 10147-10155.

Courbin, N., D. Fortin, C. Dussault, V. Fargeot, and R. Courtois. 2013. Multi-trophic resource selection function enlightens the behavioural game between wolves and their prey. *Journal of Animal Ecology* **82**:1062-1071.

Creel, S., J. Winnie, B. Maxwell, K. Hamlin, and M. Creel. 2005. Elk alter habitat selection as an antipredator response to wolves. *Ecology* **89**:3387-3397.

Crosmary, W.G., Valeix, M., Fritz, H., Madzikanda, H., and Cote, S.D. 2012. African ungulates and their drinking problems: Hunting and predation risks constrain access to water. Animal Behaviour **83**:145-153.

Cusack, J.J., A. Swanson, T. Coulson, C. Packer, C. Carbone, A. J. Dickman, M. Kosmala, C. Lintott, and J. M. Rowcliffe. 2015. Applying a random encounter model to estimate lion density from camera traps in Serengeti National Park, Tanzania. *The Journal of Wildlife Management* **79**:1014-1021.

Cusack, J. J., M. T. Kohl, M. C. Metz, T. Coulson, D. R. Stahler, D. W. Smith, and D. R. MacNulty. 2019. Weak spatiotemporal response of prey to predation risk in a freely interacting system. *Journal of Animal Ecology* DOI: 10.1111/1365-2656.12968

Eccard, J.A., J. K. Meißner, and M. Heurich. 2015. European roe deer increase vigilance when faced with immediate predation risk by Eurasian Lynx. *Ethology* **123**:30-40.

Eisenberg, C., D. E. Hibbs, W. J. Ripple, H. Salwasser. 2014. Context dependence of elk (*Cervus elaphus*) vigilance and wolf (*Canis lupus*) predation risk. *Canadian Journal of Zoology* **92**:727-736.

English, M., M. Ancrenaz, G. Gillespie, B. Goossens, S. Nathan, and W. Linklater. 2014. Foraging site recursion by forest elephants (*Elephas maximus borneensis*). *Current Zoology* **60**:551-559.

Fortin, D., and M. E. Fortin. 2009. Group-size-dependent association between food profitability, predation risk and distribution of free-ranging bison. *Animal Behaviour* **78**:887-892.

Frair, J. L., E. H. Merrill, H. L. Beyer, and J. M. Morales. 2008. Thresholds in landscape connectivity and mortality risks in response to growing road networks. *Journal of Applied Ecology* **45**:1504-1513.

Frey, S., J. T. Fisher, A. C. Burton, and J. P. Volpe. 2017. Investigating animal activity patterns and temporal niche partitioning using camera-trap data: Challenges and opportunities. *Remote Sensing in Ecology and Conservation* **3**:123-132.

Gower, C. N., R. A. Garrott, P. J. White, S. Cherry, and N. G. Yoccoz. 2008. Elk group size and wolf predation: a flexible strategy when faced with variable risk. *Terrestrial Ecology* **3**:401-422.

Greenberg, S., and T. Godin. 2015. A tool supporting the extraction of angling effort data from remote camera images. *Fisheries* **40**:276-287.

Greggor, A. L., O. Berger-Tal, D. T. Blumstein, L. Angeloni, C. Bessa-Gomes, B. F. Blackwell, C. C. St Clair, K. Crooks, S. de Silva, E. Fernández-Juricic, and S. Z. Goldenberg. 2016. Research priorities from animal behaviour for maximising conservation progress. *Trends in Ecology & Evolution* **31**:953-964.

Griffin et al. 2011. Neonatal mortality of elk driven by climate, predator phenology, and predator community composition. *Journal of Animal Ecology* **80**: 1246-1257.

Gude, J. A., R. A. Garrott, J. J. Borkowski, and F. King. 2006. Prey risk allocation in a grazing environment. *Ecological Applications* **16**:285–298.

Hamel, S., S. T. Killengreen, J. A. Henden, N. E. Eide, L. Roed-Eriksen, R. A. Ims, and N. G. Yoccoz. 2013. Towards good guidance practice in using camera-traps in ecology: influence of sampling design on validity of ecological inferences. *Methods in Ecology and Evolution* **4**:105-113.

Hebblewhite, M., and D. H. Pletscher. 2002. Effects of elk group size on predation by wolves. *Canadian Journal of Zoology* **80**:800-809.

Hebblewhite, M., E. H. Merrill, L. E. Morgantini, C. A. White, J. R. Allen, E. Bruns, L. Thurston, and T. E. Hurd. 2006. Is the migratory behavior of montane elk herds in peril? The case of Alberta's Ya Ha Tinda elk herd. *Wildlife Society Bulletin* **34**:1280-1294.

Hebblewhite, M., and E. H. Merrill. 2008. Modelling wildlife–human relationships for social species with mixed-effects resource selection models. *Journal of Applied Ecology* **45**:834-844.

Hebblewhite, M., and E. H. Merrill. 2009. Trade-offs between predation risk and forage differ between migrant strategies in a migratory ungulate. *Ecology* **90**:3445-3454.

Hebblewhite, M., and E. H. Merrill 2011. Demographic balancing of migrant and resident elk in a partially migratory population through forage–predation tradeoffs. *Oikos* **120**:1860-1870.

Hernandez, L., J.W. Laundré, and M. Gurung. 2005. From the field: Use of camera traps to measure predation risk in a puma–mule deer system. *Wildlife Society Bulletin* **33**:353-358.

Holmes, B. R., and J. W. Laundré. 2006. Use of open, edge, and forest areas by pumas (*Puma concolor*) in winter: are pumas foraging optimally? *Wildlife Biology* **12**:201-209.

Hooten, M. B., E. M. Hanks, D. S. Johnson, and M. W. Alldredge. 2013. Reconciling resource utilization and resource selection functions. *Journal of Animal Ecology* **82**:1146-1154.

Hoover, A.L., D. Liang, J. Alfaro-Shigueto, J. C. Mangel, P. I Miller, S. J. Morreale, H. Bailey, and G. L. Shillinger. 2019. Predicting residence time using a continuous-time discrete-space model of leatherback turtle satellite telemetry data. *Ecosphere* **10**:p.e02644.

Hunt, W. A., and D. Bourdin. 2016. Resource Conservation - Report from the Field 2015. Unpublished Tech. Report. Parks Canada Agency, Banff, AB. 109pp.

Jedrzejewski, W., H. Spaedtke, J. F. Kamler, B. Jedrzejewska, U. Stenkewitz. 2006. Group size dynamics of red deer in Białowieża Primeval Forest, Poland. *The Journal of Wildlife Management* **70**:1054-1059.

Jennelle, C. S., M. C. Runge and D. I. MacKenzie. 2002. The use of photographic rates to estimate densities of tigers and other cryptic mammals: a comment on misleading conclusions. *Animal Conservation Fórum* **5**:119-120.

Kapota, D., A. Dolev, D. Saltz. 2017. Inferring detailed space use from movement paths: A unifying, residence time-based framework. *Ecology and Evolution* **7**:8507-8514.

Kays, R., M. C. Crofoot, W. Jetz, and M. Wikelski. 2015. Terrestrial animal tracking as an eye on life and planet. *Science* **348**:aaa2478.

Kie, J. G. 1999. Optimal foraging and risk of predation: effects on behavior and social structure in ungulates. *Journal of Mammalogy* **80**:1114-1129.

Killeen, J., E. H. Merrill, H. Bohm, J. Berg, S. Eggeman, and M. Hebblewhite. 2015. Migration of the Ya Ha Tinda elk herd: 2002-2014. Final Report to Parks Canada.

Knopff, K. H., N. F. Webb, and M. S. Boyce. 2014. Cougar population status and range expansion in Alberta during 1991–2010. *Wildlife Society Bulletin* **38**:116-121.

Koerth, B. H., and J. C. Kroll. 2000. Bait type and timing for deer counts using cameras triggered by infrared monitors. *Wildlife Society Bulletin* **28**:630-635.

Kolowski, J. M., and T. D. Forrester. 2017. Camera trap placement and the potential for bias due to trails and other features. *PLoS one* **12**:e0186679.

Kortello, A. D., T. E. Hurd, and D. L. Murray. 2007. Interactions between cougars (*Puma concolor)* and gray wolves (*Canis lupus*) in Banff National Park, Alberta. *Ecoscience* **14**:214-222.

Kusler, A., L. M. Elbroch, H. Quigley, and M. Grigione. 2017. Bed site selection by a subordinate predator: an example with the cougar (*Puma concolor*) in the Greater Yellowstone Ecosystem. *Journal of Life and Environmental Sciences* **5**:e4010.

Ladle, A., T. Avgar, M. Wheatley, and M. S. Boyce. 2017. Predictive modelling of ecological patterns along linear-feature networks. *Methods in Ecology and Evolution* **8**:329-338.

Latombe, G., D. Fortin, and L. Parrott. 2014. Spatio-temporal dynamics in the response of woodland caribou and moose to the passage of grey wolf. *Journal of Animal Ecology* **83**:185-198.

Laundré, J. W., and L. Hernández. 2003. Winter hunting habitat of pumas Puma concolor in northwestern Utah and southern Idaho, USA. *Wildlife Biology* **9**:123-130.

Laundré, J. W., L. Hernández, and K. B. Altendorf. 2001. Wolves, elk, and bison: reestablishing the "landscape of fear" in Yellowstone National Park, U.S.A. *Canadian Journal of Zoology* **79**:1401-1409.

Liley, S., S. Creel. 2007. What best explains vigilance in elk: characteristics of prey, predators, or the environment? *Behavioral Ecology* **19**:245-254.

Lone, K., L. E. Loe, T. Gobakken, J. D. Linnell, J. Odden, J. Remmen, and A. Mysterud. 2014. Living and dying in multi-predator landscape of fear: Roe deer are squeezed by contrasting pattern of predation risk by lynx and humans. *Oikos* **123**:621-651.

Lucas, T. C., E. A. Moorcroft, R. Freeman, J. M. Rowcliffe, and K. E. Jones. 2015. A generalised random encounter model for estimating animal density with remote sensor data. *Methods in Ecology and Evolution* **6**:500-509.

Mao, J. S., M. S. Boyce, D. W. Smith, F. J. Singer, D. J. Vales, J. M. Vore, and E. H. Merrill. 2005. Habitat selection by elk before and after wolf reintroduction in Yellowstone National Park. *Journal of Wildlife Management* **69**:169-1707.

Marzluff, J. M., J. J. Millspaugh, P. Hurvitz, and M. S. Handcock. 2004. Relating resources to a probabilistic measure of space use: forest fragments and Steller's jays. *Ecology* **85**:1411-1427.

Martin, J., S. Benhamou, K. Yoganand, and N. Owen-Smith. 2015. Coping with spatial heterogeneity and temporal variability in resources and risks: adaptive movement behaviour by a large grazing herbivore. *PloS one* **10**:e0118461.

McCoy, J. C., S. S. Ditchkoff, and T. D. Steury. 2011. Bias associated with baited camera sites for assessing population characteristics of deer. *Journal of Wildlife Management* **75**:472-477.

McPhee, H. M., N. F. Webb, and E. H. Merrill. 2012. Hierarchical predation: wolf (*Canis lupus*) selection along hunt paths and at kill sites. *Canadian Journal of Zoology* **90**:555-563.

Metz, M.C., Emlen, D.J., Stahler, D.R., MacNulty, D.R., Smith, D.W., and M. Hebblewhite. 2018. Predation shapes the evolutionary traits of cervids. Nature **2**: 1619-1625.

Middleton, A. D., M. J. Kauffman, D. E. McWhirter, J. G. Cook, R. C. Cook, A. A. Nelson, M. D. Jimenez, and R. W. Klaver. 2013. Animal migration amid shifting patterns of phenology and predation: lessons from a Yellowstone elk herd. *Ecology* **94**:1245-1256.

Millspaugh, J. J., R. M. Nielson, L. McDonald, J. M. Marzluff, R. A. Gitzen, C. D. Rittenhouse, M. W. Hubbard, and S. L. Sheriff. 2006. Analysis of resource selection using utilization distributions. *Journal of Wildlife Management* **70**:384-395.

Moeller, A. K., P. M. Lukacs, and J. S. Horne. 2018. Three novel methods to estimate abundance of unmarked animals using remote cameras. *Ecosphere* **9**:e02331.

Montgomery, R. A., G. J. Roloff, and J. J. Millspaugh. 2012. Variation in elk responses to roads by season, sex, and road type. *The Journal of Wildlife Management* **77**:313-325.

Parsons, A. W., T. Forrester, W. J. McShea, M. C. Baker-Whatton, J. J. Millspaugh, and R. Kays. 2017. Do occupancy or detection rates from camera traps reflect deer density? *Journal of Mammalogy* **98**:1547-1557.

Proffitt, K. M., J. L. Grigg, K. L. Hamlin, and R. A. Garrott. 2009. Contrasting effects of wolves and human hunters on elk behavioral responses to predation risk. *The Journal of Wildlife Management* **73**:345-356.

Proffitt, K.M., N. Anderson, P. Lukacs, M. M. Riordan, J. A. Gude, J. Shamhart. 2015. Effects of elk density on elk aggregation patterns and exposure to brucellosis. *Journal of Wildlife Management* **79**:373–383.

Prokopenko, C. M., M. S. Boyce, and T. Avgar. 2016. Extent-dependent habitat selection in a migratory large herbivore: road avoidance across scales. *Landscape Ecology* **31**:1-13.

Prokopenko, C. M., M. S. Boyce, and T. Avgar. 2017. Characterizing wildlife behavioural responses to roads using integrated step selection analysis. *Journal of Applied Ecology* **54**:470-479.

Robinson, B. G., M. Hebblewhite, and E. H. Merrill. 2010. Are migrant and resident elk (*Cervus elaphus*) exposed to similar forage and predation risk on their sympatric winter range? *Oecologia* **164**:265-275.

Robinson, B. G., and E. H. Merrill. 2013. Foraging–vigilance trade-offs in a partially migratory population: comparing migrants and residents on a sympatric range. *Animal Behaviour* **85**:849-856.

Rosatte, R. 2017. Home ranges and movements of elk (*Cervus canadensis*) restored to southern Ontario, Canada. *The Canadian Field-Naturalist* **130**:320-331.

Rowcliffe, J. M., J. Field, S. T. Turvey, C. Carbone. 2008. Estimating animal density using camera traps without the need for individual recognition. *Journal of Applied Ecology* **45**:1228-1236.

Royle, J. A., R. B. Chandler, R. Sollmann, and B. Gardner. 2013. Spatial capture-recapture. Academic Press. Waltham, Massachusetts, USA.

Schlägel, U.E., Merrill, E.H., and Lewis, M.A. 2017. Territory surveillance and prey management: Wolves keep track of space and time. *Ecology and Evolution* **7**: 8388-8405.

Seidel, D. P., and M. S. Boyce. 2015. Patch-use dynamics by a large herbivore. *Movement Ecology* **3**:7.

Signer, J., J. Fieberg, and T. Avgar. 2017. Estimating utilization distributions from fitted step-selection functions. *Ecosphere* **8**:e01771.

Steenweg, R., J. Whittington and M. Hebblewhite. 2015. Canadian Rockies Remote Camera Multi-Species Occupancy Project: Examining trends in carnivore populations and their prey using remote cameras in Banff, Jasper, Kootenay, Yoho and Waterton Lakes National Parks. Final Report. March 31, 2015. University of Montana. 88pp.

Steenweg, R., J. Whittington, M. Hebblewhite, A. Forshner, B. Johnston, D. Petersen, B. Shepherd, P. M. and Lukacs. 2016. Camera-based occupancy modelling at large scales: Power to detect trends in grizzly bears across the Canadian Rockies. *Biological Conservation* **201**:192-200.

Sur, M., A. K. Skidmore, K. M. Exo, T. Wang, B. J. Ens, and A. G. Toxopeus. 2014. Change detection in animal movement using discrete wavelet analysis. *Ecological Informatics* **20**:47-57.

Thaker, M., A. T. Vanak, C. R. Owen, M. B. Ogden, S. M. Niemann, and R. Slotow. 2011. Minimizing predation risk in a landscape of multiple predators: Effects on the spatial distribution of African ungulates. *Ecology* **92**:398-407.

Therneau, T. M., and Grambsch, P. M. 2013. Modeling survival data: Extending the Cox model. Springer Science & Business Media.

Tomkiewicz, S. M., M. R. Fuller, J. G. Kie, and K. K. Bates. 2010. Global positioning system and associated technologies in animal behaviour and ecological research. *Philosophical Transactions of the Royal Society B: Biological Sciences* **365**:2163-2176.

Valeix, M., Loveridge, M.J., CHamaille-Jammes, S., Davidson, Z., Murindagomo, F. Fritz, H. *et al* (2009a). Behavioral adjustments of African herbuvores to predation risk by lion: Spatiotemporal variations influence habitat use. *Ecology* **90**: 23-30.

Van Moorter, B., C. M. Rolandsen, M. Basille, and J. M. Gaillard. 2016. Movement is the glue connecting home ranges and habitat selection. *Journal of Animal Ecology* **85**:21-31.

Wikenros, C., D. P. Kuijper, R. Behnke, and K. Schmidt. 2015. Behavioural responses of ungulates to indirect cues of an ambush predator. *Behaviour* **152**:1019-1040.

Wisdom, M. J., H. K. Preisler, L. M. Naylor, R. G. Anthony, B. K. Johnson, and M. M. Rowland. 2018. Elk responses to trail-based recreation on public forests. *Forest Ecology and Management* **411**:223-233.

Wolf, M., J. Frair, E. H. Merrill, and P. Turchin. 2009. The attraction of the known: the importance of spatial familiarity in habitat selection in wapiti (*Cervus elaphus*). *Ecography* **32**:401-410.

Yau, K.K.W. 2001. Multilevel models for survival analysis with random effects. *Biometrics* **57**:96-102.

Appendix 1. Distribution of cameras among open-canopy, closed-canopy, and edge cells and various distances from human activity. Open areas included all grassland, herbaceous, and burned habitats and all forested interiors (*e.g.* conifer, deciduous, mixed) were categorized as closed areas. Forest edges were limited to a 20-m buffer across the interface between open and closed areas.

	Distance to ranch buildings			
Vegetation type	0–1 km	>1–3 km	>3–7 km	**TOTAL**
Closed canopy	2	4	7	**13**
Open canopy	2	5	8	**15**
Edge	3	5	8	**16**
TOTAL	**7**	**14**	**23**	**44**

Appendix 2. Number of cameras that captured each focal species and total number of events during winter (1 Dec – 30 Apr) and summer (1 June – 15 Sept) in 2017 and 2018.

	No. cameras	No. of events		
Species	w/ events	Winter	Summer	**TOTAL**
Elk (*Cervus elaphus*)	42	418	877	**1295**
Wolf (*Canis lupus*)	24	78	78	**156**
Grizzly (*Ursus arctos*)	16	8	55	**63**
Cougar (*Puma concolor*)	10	13	15	**28**

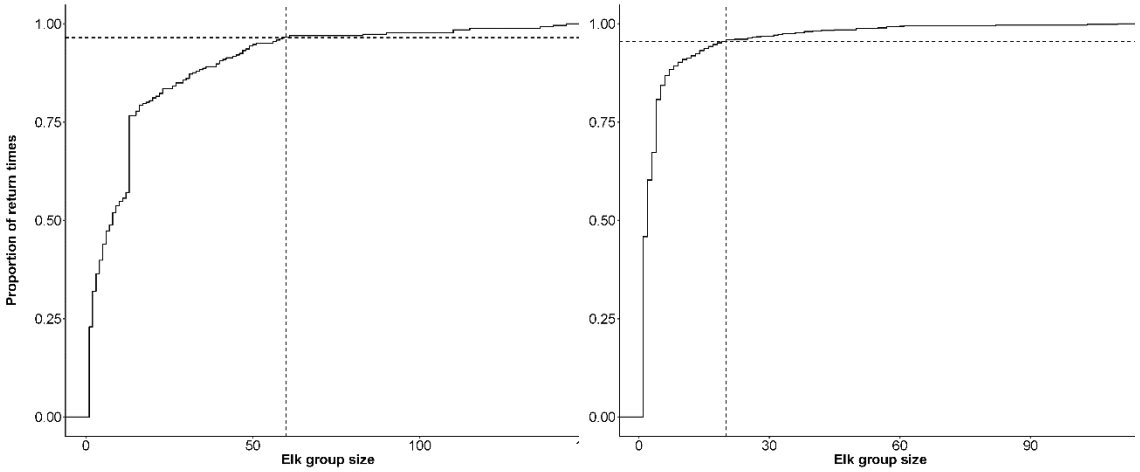

Appendix 3. Cumulative distribution of elk group sizes during winter (left) and summer (right). When larger groups were present, we limited group sizes to the maximum herd count estimated from 95% (dotted lines) of all other elk observations in each season. In winter, 95% of elk events had less than 60 individuals with a mean of 8 (14.8 ± 1.4 [mean ± SE]). In summer, 95% of elk events had less than 20 individuals within a mean of 2 (4.8 ± 0.4).

Appendix 4. Pairwise comparisons of proportions of locations in the camera area (top) and mean home range sizes (bottom) between summer periods using a Wilcoxon Rank-Sum test.

	***P* values**		
Proportion of locations	Early	Late	Middle
Late	>0.99	--	--
Middle	>0.99	>0.99	--
Very early	0.003	0.012	0.004
	***P* values**		
Home range size	Early	Late	Middle
Late	< 0.001	--	--
Middle	> 0.99	< 0.001	--
Very early	< 0.001	0.25	< 0.001

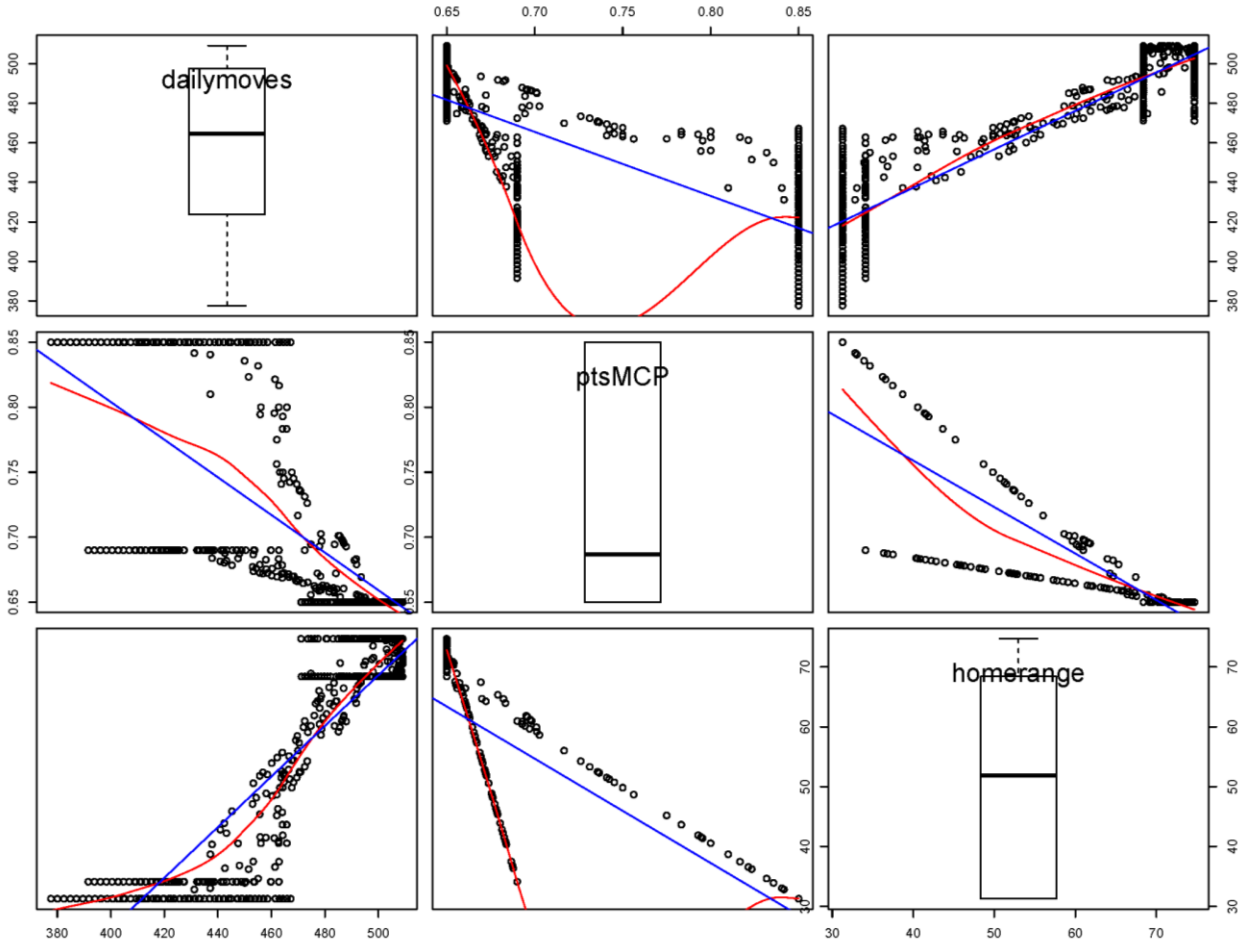

Appendix 5. Correlations among elk movement and distribution metrics. The mean daily movement rate across days between elk events (dailymoves) was highly correlated with weighted averages of the proportion of locations (ptsMCP) in the camera area (r = –0.69, P < 0.001) and mean home range sizes (r = 0.91, P < 0.001). Mean proportion of locations were also highly correlated with home range sizes (r = –0.79, P < 0.001). Values are fitted with a smoothed (LOWESS; in red) and least squares line (blue).

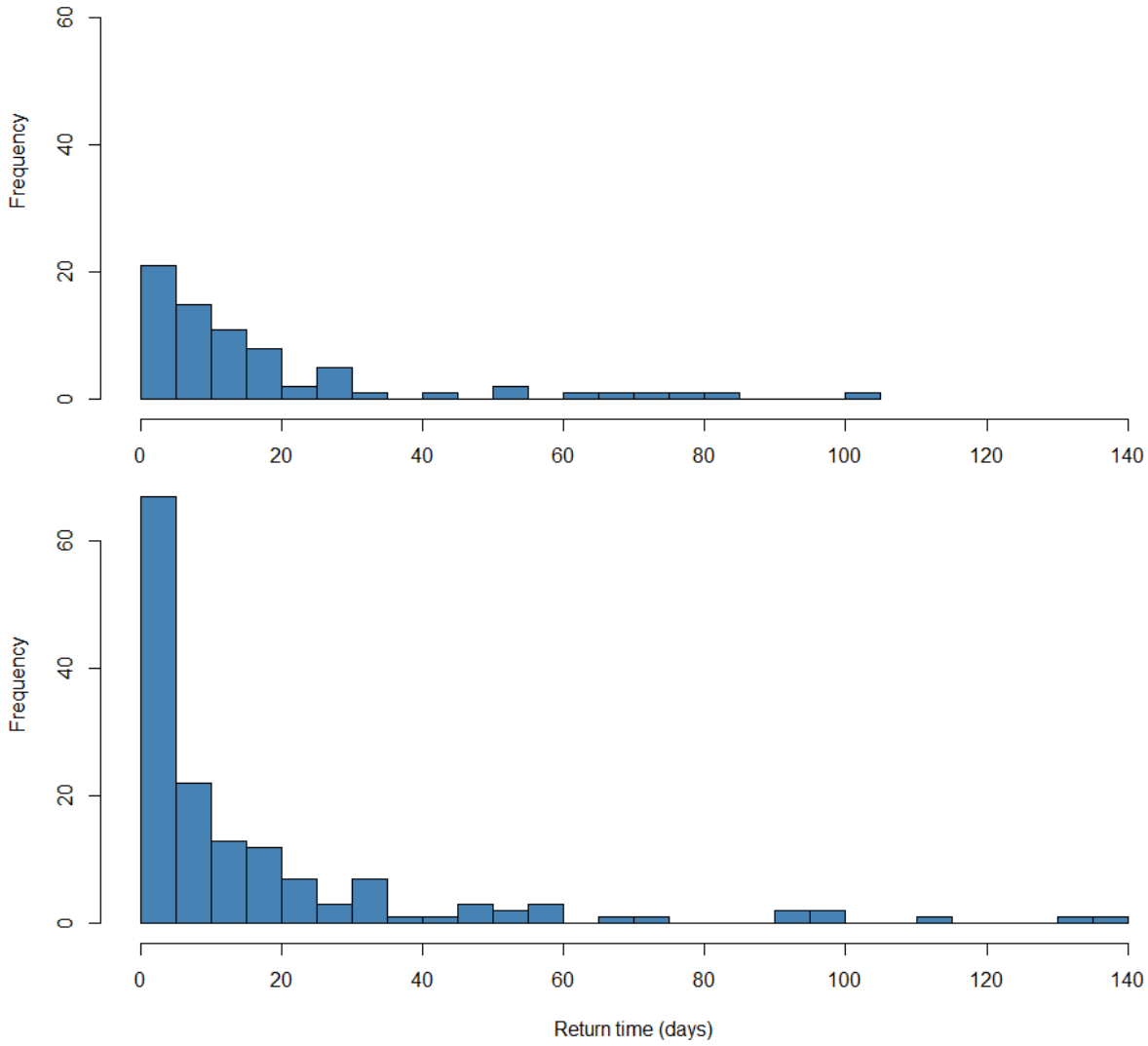

Appendix 6. Histogram of revisit times in winter for 2017 (top; n = 91) and 2018 (bottom; n = 258). Distributions include all observations from cameras operating during both winters that detected elk (n = 17). A Kolmogorov-Smirnov indicates that revisit times from 2017 do not differ from 2018 (D = 0.166, p = 0.139

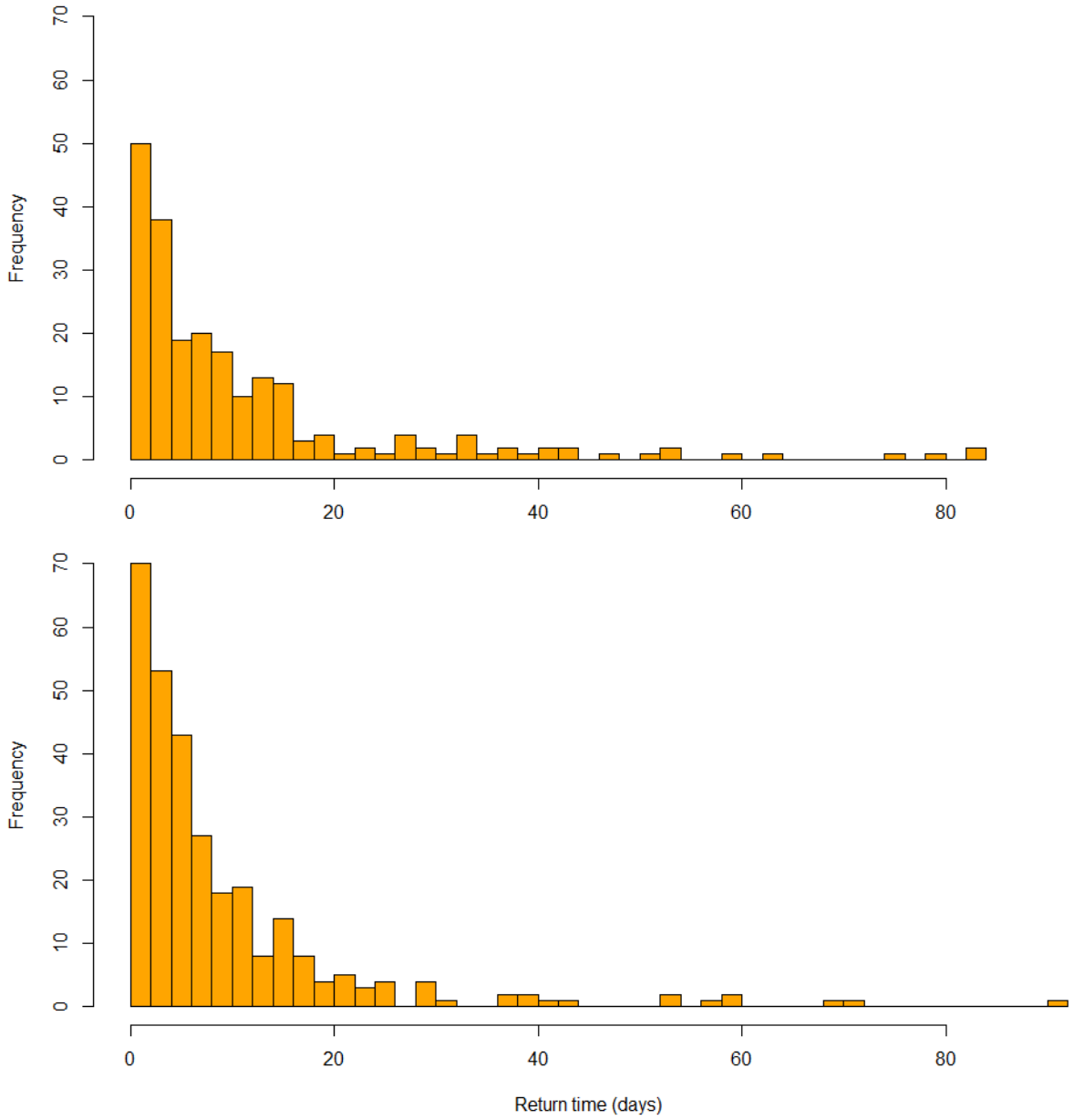

Appendix 7. Histogram of revisit times in summer for 2017 (top; n = 342) and 2018 (bottom; n = 536). Distributions include all observations from cameras operating during both summers that detected elk (n = 28). A Kolmogorov-Smirnov indicates that revisit times from 2017 do not differ from 2018 (D = 0.107, p = 0.114).

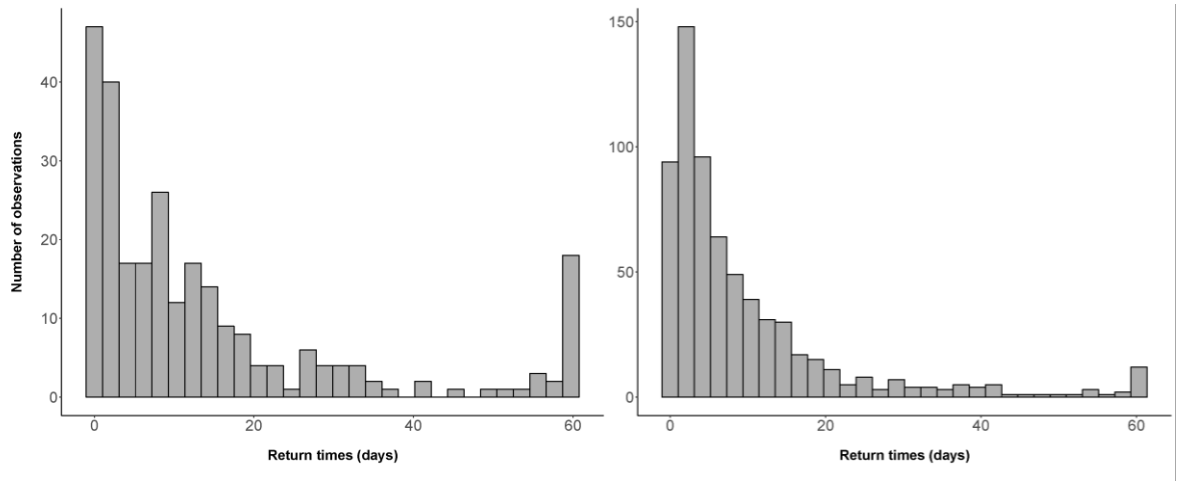

Appendix 8. Histogram of all revisit times used for modelling during winter (left) and summer (right). We used a 60-day revisit threshold for right censoring elk revisit times, which removed only 14 (5.3%) elk revisit times in winter and 11 (1.6%) in summer, but allowed us to meet the assumptions of the Cox proportional hazard model in all the models presented.

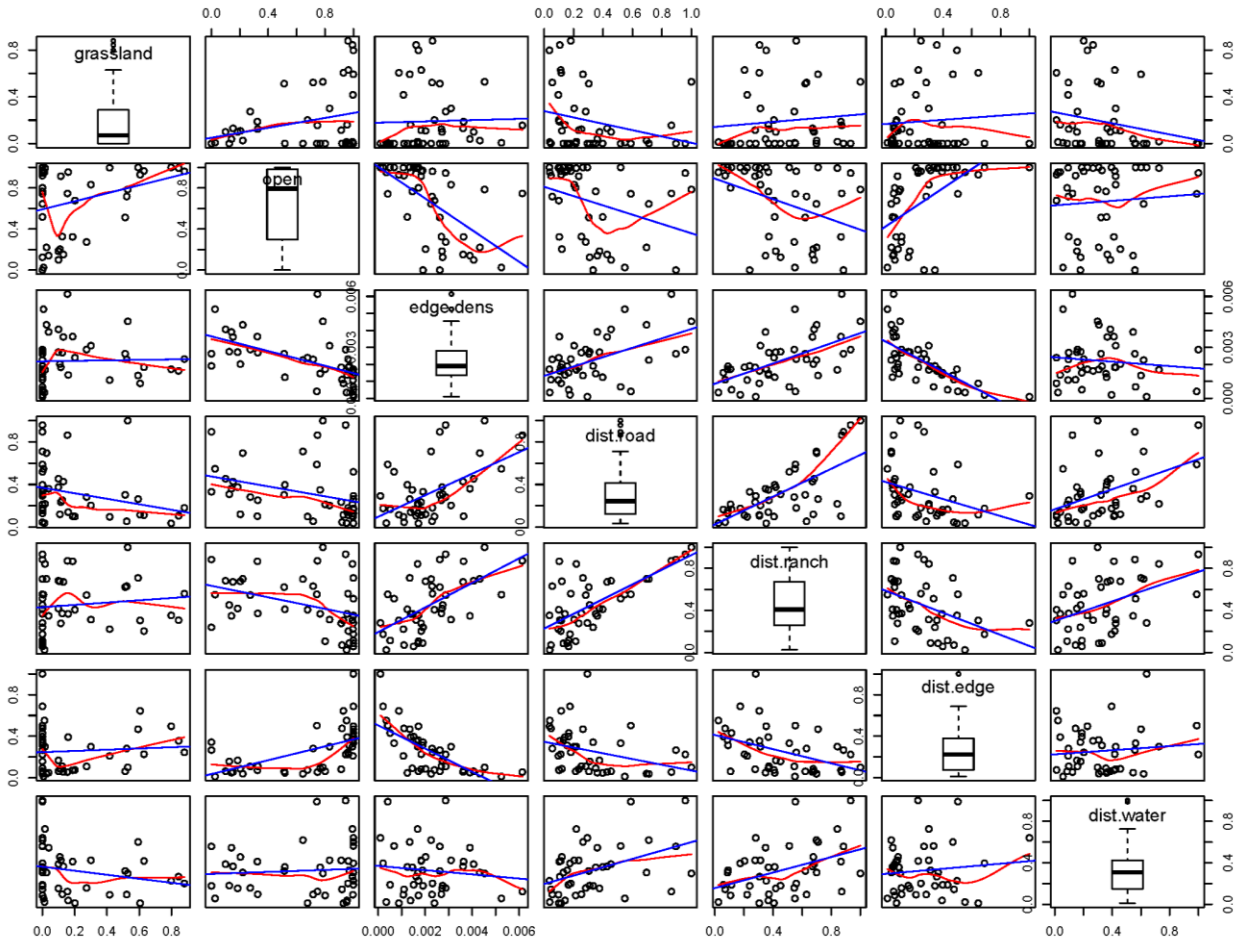

Appendix 9. Correlation matrix of fixed site characteristics at remote cameras. Distance to the ranch buildings was significantly highly correlated with distance to road ($r = 0.68$, $P < 0.001$) and edge density ($r = 0.59$, $P < 0.001$). Distance to edge was highly correlated with edge density ($r = 0.7$, $P < 0.001$) and proportion of open habitat within 300 m ($r = 0.56$, $P < 0.001$). Values are fitted with a smoothed (LOWESS; in red) and least squares line (blue).

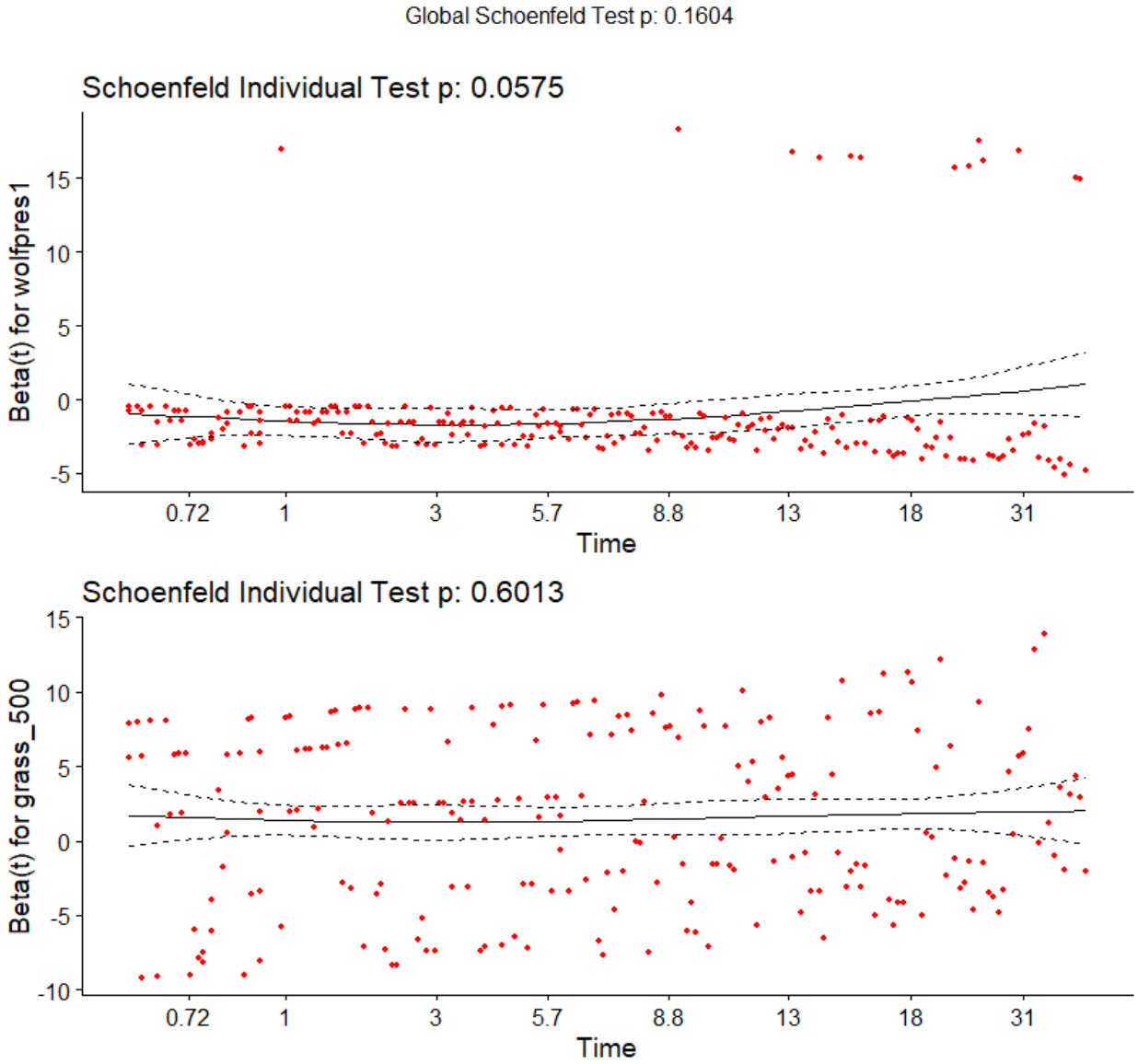

Appendix 10. Plots of scaled Schoenfeld residuals (y-axis) against (transformed) event times (x-axis) for a mixed-effects Cox proportional hazards model fitted to elk revisit times in winter (n = 266) with 2 predictors [wolf presence (0/1) and nearby grassland area (%)]. Each predictor has a smoothed LOESS curve (solid black) overlaid with a 95% confidence interval (black dashed curves). We found no obvious trends in the residual plots for each predictor (*i.e.*, residuals are independent of time), which is further supported by the corresponding Grambsch–Therneau tests ($P = 0.056 – 0.601$). A global test is also reported ($P = 0.16$).

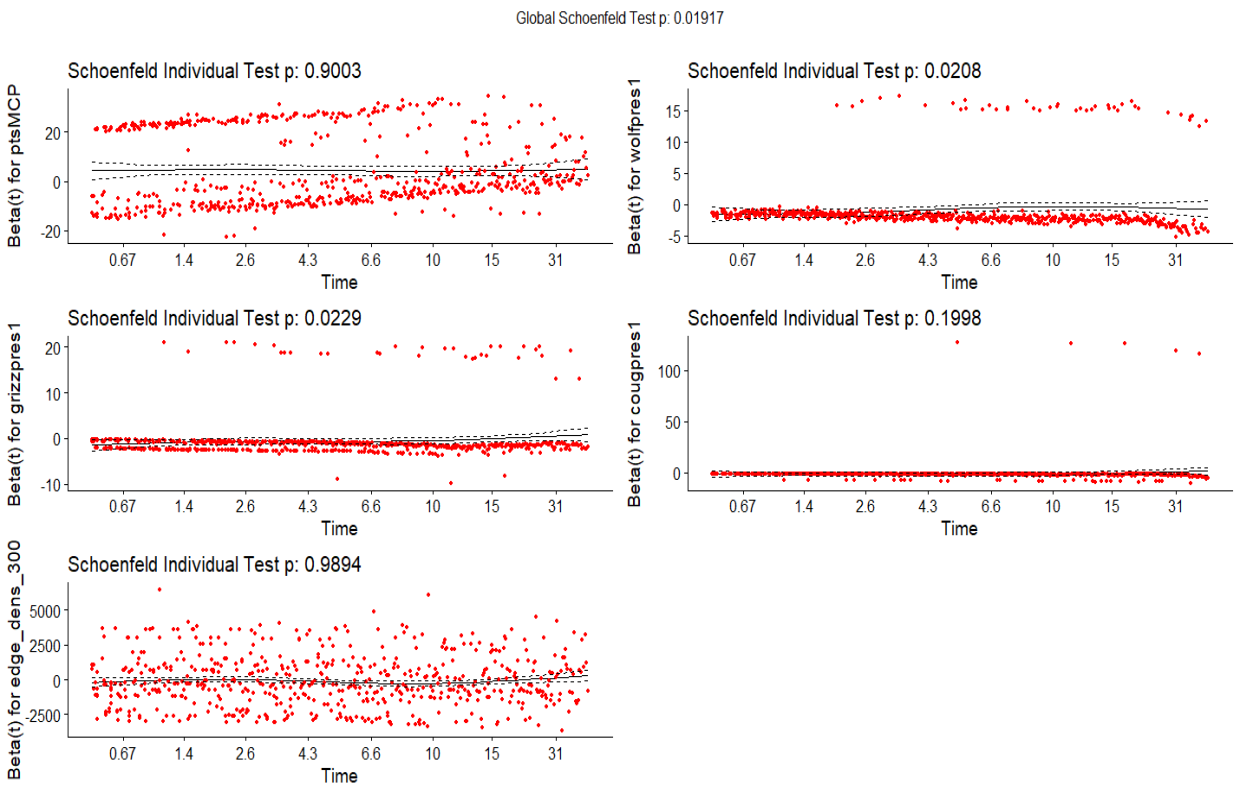

Appendix 11. Plots of scaled Schoenfeld residuals (y-axis) against (transformed) event times (x-axis) for a mixed-effects Cox proportional hazards model fitted to elk revisit times in summer (n = 665) with 5 predictors [prop.pts (%), wolf, grizzly, and cougar presence (0/1), and edge density (km/km^2)]. Each predictor has a smoothed LOESS curve (solid black) overlaid with a 95% confidence interval (black dashed curves). We found no obvious trends in the residual plots for each predictor (*i.e.*, residuals are independent of time), which is further supported by the corresponding Grambsch–Therneau tests seen above each plot (P = 0.02 – 0.99). A global test is also reported (P = 0.02). Due to large sample sizes, we used $P < 0.01$ as a conservative approach for rejecting significant deviations from 0 in the slopes of fitted residual curves. Visual inspection of residuals for wolf and grizzly presence reveals they are symmetric about 0 until approximately 20 days (t = 15–31), when a predator's influence on elk revist times might be expected to decrease.

Appendix 12. Model selection results based on AIC for predicting revisit times of elk at remote camera sites across the Ya Ha Tinda during winter (1-December to 30-April). All models include a random effect for location ID. The top model is shown in bold. Variable definitions in Table 2.

Model	K	AIC	ΔAIC	AIC Wt.
Wolf + grassland	**3**	**2066.79**	**0**	**0.26**
Wolf + grassland + dist.road	**4**	**2068.03**	**1.25**	**0.14**
Wolf + grassland + wolf×grassland	**4**	**2068.53**	**1.74**	**0.11**
Wolf + grassland + edge.dens	4	2068.83	2.04	0.093
Wolf + grassland + group.size	4	2068.83	2.05	0.093
Wolf + grassland + dist.road + wolf×dist.road	5	2068.85	2.07	0.092
Wolf + grassland + dist.road + wolf×grassland	5	2069.90	3.11	0.055
Wolf + grassland + dist.road + group.size	5	2070.05	3.27	0.051
Wolf + grassland + herd size + wolf×herdsize	5	2070.43	3.64	0.042
Wolf + grassland + herd size + wolf×grassland	5	2070.59	3.81	0.039
Wolf + grassland + dist.road+ group.size + wolf×group.size	6	2071.58	4.79	0.024
Wolf + dist.road	3	2075.65	8.86	0.0031
Wolf + dist.road + wolf×dist.road	4	2076.86	10.08	0.0017
Grassland	2	2078.27	11.48	0.00083
Wolf + edge.dens	3	2078.48	11.69	0.00075
Grassland + group.size	3	2080.20	13.42	0.00032
Wolf	2	2081.17	14.39	0.00019
Wolf + herd size	3	2083.22	16.43	$7.0*10^{-5}$
Dist.road	2	2090.83	24.05	$1.6*10^{-6}$
Location ID (null)	2	2096.09	29.30	$1.1*10^{-7}$

Appendix 13. Summary of model selection results based on AIC for predicting revisit times of elk at remote camera sites across the Ya Ha Tinda during summer (1-June to 15-Sept). All models include a random effect for location ID. Top model is shown in bold.

Model	K	AIC	ΔAIC	AIC Wt.
Prop.pts + wolf + grizzly + cougar + edge.dens	**6**	**6514.02**	**0**	**0.41**
Prop.pts + wolf + grizzly + cougar + edge.dens + group.size	7	6516.05	2.03	0.15
Prop.pts + wolf + grizzly + cougar + dist.road	6	6516.49	2.47	0.12
Prop.pts + wolf + grizzly + cougar + group.size	6	6517.09	3.07	0.087
Prop.pts + wolf + grizzly + cougar + group.size + dist.ranch	7	6517.79	3.77	0.062
Prop.pts + wolf + grizzly + cougar + group.size + edge.dens + group.size×edge.dens	8	6518.10	4.08	0.053
Prop.pts + wolf + grizzly + cougar + group.size + dist.road	7	6518.45	4.43	0.044
Prop.pts + wolf + grizzly	4	6520.44	6.42	0.016
Prop.pts + predpres + group.size + edge.dens	5	6520.87	6.86	0.013
Prop.pts + wolf + grizzly + dist.road	5	6521.88	7.86	0.0080
Prop.pts + predpres + group.size	4	6521.95	7.93	0.0077
Prop.pts + wolf + grizzly + group.size	5	6522.30	8.28	0.0064
Prop.pts + predpres + group.size + edge.dens + predpres×edge.dens	6	6522.90	8.88	0.0048
Prop.pts + predpres + group.size + edge.dens + predpres×group.size	6	6522.90	8.88	0.0048
Prop.pts + predpres + group.size + bullpres	5	6523.61	9.5	0.0034
Prop.pts + wolf + grizzly + group.size + dist.road	6	6523.78	9.76	0.0031
Prop.pts + predpres + group.size + predpres×group.size	5	6523.98	9.96	0.0028
Prop.pts + wolf + grizzly + group.size + open	6	6524.26	10.24	0.0024
Prop.pts + wolf	3	6529.97	15.95	0.00014
Prop.pts + wolf + dist.road	4	6530.95	16.92	< 0.001
Prop.pts + wolf + group.size	4	6531.75	17.73	< 0.001
Prop.pts + group.size + calves + group.size×calves	5	6548.98	34.96	< 0.001
Prop.pts	2	6557.541	43.52	< 0.001

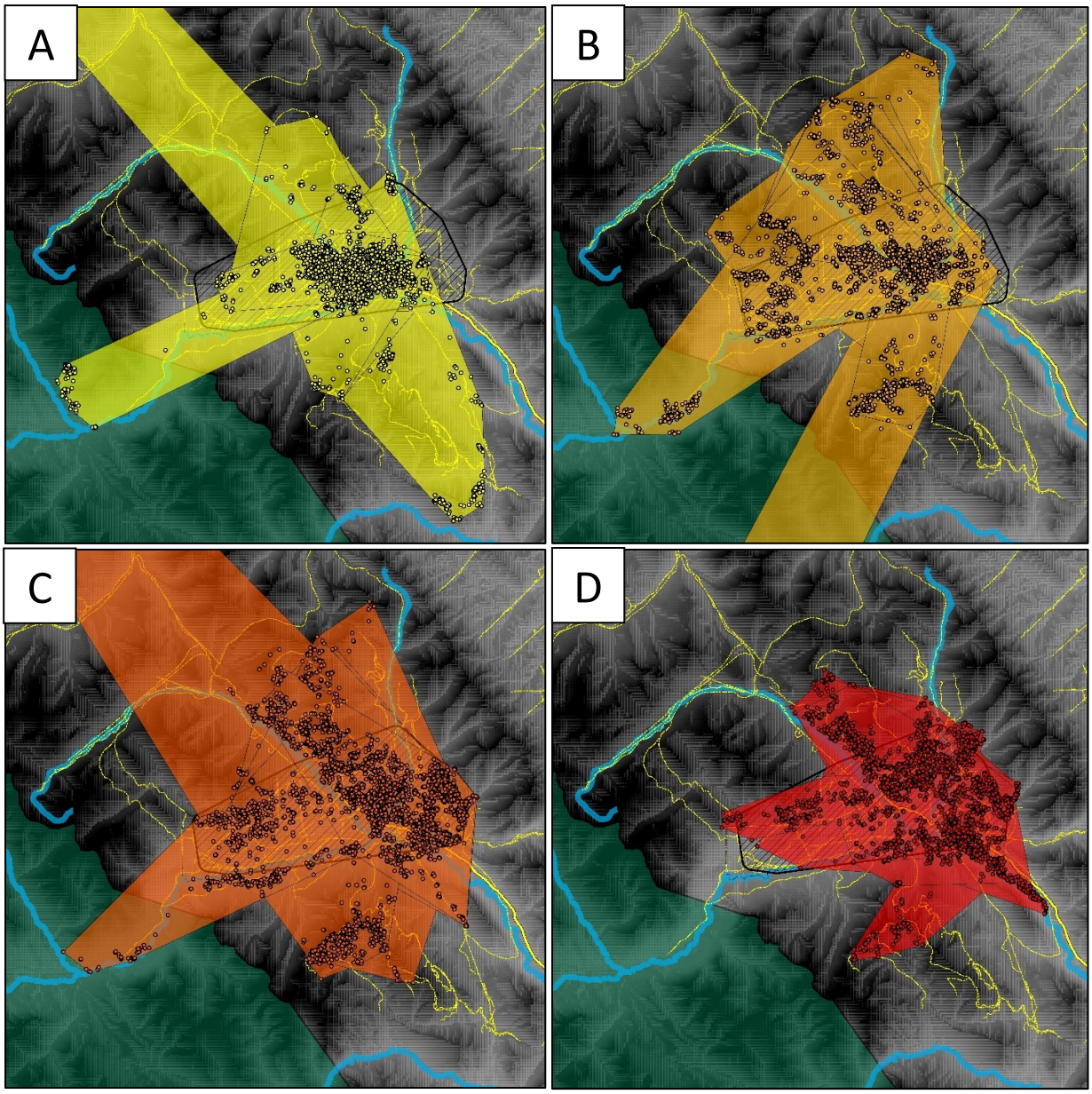

Appendix 14. Minimum convex polygons and individual locations (n = ~12,000 locations per period) of GPS-collared resident elk (n =21) monitored throughout the (A) very early [1 June – 25 June], (B) early [26 June – 25 July], (C) middle [26 July – 25 Aug], and (D) late [26 Aug – 15 Sept] summer periods in 2017.